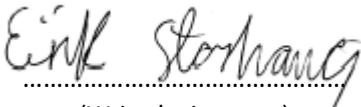




Faculty of Science and Technology

MASTER THESIS

Study program/Specialization: Construction and Materials/Offshore constructions	Vårsemesteret, 2016 <u>Open</u> / Restricted access
Writer: Eirik Storhaug	 (Writer's signature)
Faculty supervisor: Hirpa G. Lemu	
External supervisor(s): Arne B. Nysæther	
Thesis title: Optimal design for projectile and blast protection during pressure testing	
Credits (ECTS): 30	
Key words: Pressure testing, Risk analysis, Wall penetration, potential energy to kinetic energy during failure, design safety walls	Pages: 86 + 14p Enclosure Stavanger, 15.06/2016

Preface

There is no specific regulation in Norway that deal with safety during pressure testing. The regulations on pressure testing is unclear in terms of safety. In addition, the accompanying literature gives a poor definition of different hazards involved in pressure testing and lack methods to estimate the severity of these hazards.

The candidate shall perform an analysis of risk during hydrostatic pressure testing at the new workshop for T.D.W. Offshore Services (TDW). This involve identification of hazards, and estimating the severity of these events through calculations. Further, the candidate shall give suggestions to mitigating measures to reduce the risk to an acceptable level. The risk-reducing effect of these measures should be determined through calculations and analyzes.

The thesis will be written at Institute of Construction and Materials at University in Stavanger. The research is conducted in collaboration with TDW who defined the research problem.

The start date of the thesis is the 01. February 2016 and the submission date the 15. June 2016. Within this time period, the candidate should have given a clear presentation of the work, results and conclusions. The candidate should during the report give a personal contribution to the solution of the issue described in the thesis.

Table of contents

1	INTRODUCTION.....	1
1.1	<i>Background</i>	1
1.2	<i>Objective</i>	1
1.3	<i>Scope of work</i>	2
2	SAFETY REQUIREMENTS DURING PRESSURE TESTING.....	3
3	ENERGY STORED IN PRESSURIZED VESSEL.....	4
4	RISK ANALYSIS.....	5
4.1	<i>Risk</i>	5
4.2	<i>Description of risk</i>	6
4.3	<i>Severity, Probability and uncertainty</i>	6
4.4	<i>Hazard</i>	8
4.5	<i>Risk acceptance criteria</i>	9
4.6	<i>ALARP</i>	11
5	ASSESSMENT OF HAZARDS THROUGH CALCULATIONS.....	12
5.1	<i>Pressure wave</i>	15
5.2	<i>Water jet</i>	16
5.2.1	Liquid discharge rates through a small orifice.....	18
5.2.2	Dispersion of Jet.....	18
5.3	<i>Small, high velocity projectiles</i>	19
5.4	<i>Plug discharge</i>	20
6	SAFETY WALLS THEORY.....	22
6.1	<i>Impulse force</i>	22
6.2	<i>Bounce back</i>	24
6.3	<i>Coefficient of Residual energy</i>	24
6.4	<i>Wall penetration by projectile</i>	25
6.4.1	Adeli and Amin formula for penetration.....	27
6.4.2	Hughes formula for penetration.....	27
6.4.3	Forrestal formula for penetration.....	28
6.4.4	Range of empirical formulas.....	29
6.4.5	Analytical model of penetration.....	30
6.5	<i>Wall perforation by projectile</i>	31
6.5.1	NDRC formula for perforation thickness.....	32
6.5.2	Chang formula for perforation.....	32
6.5.3	Hughes formula for perforation.....	32
6.5.4	Adeli and Amin formula for perforation.....	32
6.6	<i>Wall scabbing</i>	33
6.6.1	NDRC formula for scabbing.....	34
6.6.2	Chang formula for scabbing.....	34
6.6.3	Hughes formula for scabbing.....	34
6.6.4	Adeli and Amin formula for scabbing.....	34
6.7	<i>Review of the formulas</i>	35
7	TEST OF PROJECTILE DISCHARGE.....	36
7.1	<i>Testing procedure</i>	37

7.2	<i>Equipment</i>	38
7.3	<i>Preliminary calculations</i>	39
7.3.1	Ultimate shear strength Brass M3-pins.....	39
7.3.2	Calculation of potential energy in the vessel	41
7.3.3	Calculation of trajectory.....	42
7.4	<i>Test results</i>	43
7.5	<i>Discussion of results</i>	44
8	TOTAL ENERGY DURING PRESSURE TESTING.....	47
8.1	<i>200 bar FAT-test Smartplug</i>	47
8.2	<i>500 bar structural test Smartlay</i>	48
8.3	<i>Pressure wave result</i>	49
8.4	<i>Water jet result</i>	49
9	DESIGN OF SAFETY WALLS.....	51
9.1	<i>Choice of materials</i>	51
9.1.1	Steel barrier	51
9.1.2	Concrete barrier.....	57
9.1.3	Composite barrier	60
9.2	<i>Fixed safety walls</i>	61
9.2.1	Penetration of fixed safety walls.....	62
9.2.2	Perforation of fixed Safety walls	64
9.3	<i>Existing Safety walls</i>	65
9.3.1	Penetration	66
9.3.2	Scabbing.....	68
9.3.3	Shear forces	69
9.4	<i>Steel safety walls</i>	70
9.4.1	Energy absorption during impact.....	71
9.4.2	Effect of large projectiles on steel wall	72
9.4.3	Resistance to shear forces.....	74
9.5	<i>Composite safety walls</i>	76
9.6	<i>Existing safety walls 1</i>	76
9.7	<i>Existing safety walls 2</i>	77
10	DISCUSSION OF DESIGN	78
11	CONCLUSION & FURTHER WORK.....	81
11.1	<i>Conclusion</i>	81
11.2	<i>Recommendations for further work</i>	83
12	REFERENCES	84

Summary

The thesis identifies the main hazards in hydrostatic pressure testing as pressure wave, water jet, burst of water hose, fragment and projectile discharge as well as ejection of plug or end section.

A test, where a pressurized vessel ejected a projectile, was conducted as part of the thesis. The aim of this test was to find the relationship between potential energy inside pressure vessel and kinetic energy in a discharged projectile. The results showed that the Baker formula together with the elastic energy of the expanded pipe, gave a good representation of the kinetic energy.

Based on the results from the test, a risk analysis concerning pressure testing at TDW is made. The analysis involves hazards assessment through calculations. Existing safety walls are analyzed and mediating measures to lower the risk to an acceptable level are proposed.

An assessment of the safety barriers concluded that only fragments and projectiles or plug and end section could breach the first two safety barriers. Fragments and projectiles will most likely perforate the safety walls, while a plug or end section will probably exceed the shear and moment capacities in the safety wall. The pressure wave, water jet and burst of water hose would most likely be confined by the first barrier.

For the vessels and pressure tests considered in this paper, the thesis suggests three safety barriers to reduce the risk to an acceptable level. First safety barrier should be an existing safety wall. The second safety barrier is a closed off area between the first and third safety barrier. The third and last safety barrier is either an existing safety wall or a steel safety wall.

To improve the existing safety wall, a steel plate should be attached behind the wall. The steel plate will increase the shear strength of the wall as well as preventing sections of the wall to collapse during perforation of projectile.

The calculations indicate that either a steel safety wall or the existing safety wall can be perforated by smaller projectiles. Because of small projectile diameter and large velocity, the wall at impact location will undergo a local deformation. This will lead to smaller plastic deformation and less energy is absorbed by the wall.

Large projectile will create a global effect on the walls. These projectiles will not perforate the wall, but instead apply large axial and moment forces to the wall. To improve the walls resistance against axial and bending loads, the safety walls should be bolted to the floor.

Figure list

- Figure 1 Model of two plugs inside the pipe 1
- Figure 2 Event tree of pipe rupture..... 7
- Figure 3 Operator removes a valve under pressure 9
- Figure 4 Hoop stress and longitudinal stress in a pipe 13
- Figure 5 Different scenarios of failure of a pipe 14
- Figure 6 Pipe collapse with shock wave..... 15
- Figure 7 Water jet during projectile test..... 16
- Figure 8 Projectile used during testing 19
- Figure 9 Decomposition of forces during impact..... 23
- Figure 10 Ball bouncing 24
- Figure 11 Spherical model during impact 25
- Figure 12 Penetration of safety walls 31
- Figure 13 A two-stage perforation model 33
- Figure 14 Model of test-assembly 36
- Figure 15 Projectile with pins: 37
- Figure 16 Test-assembly with protective pipe..... 37
- Figure 17 Captions of projectile discharge during test..... 43
- Figure 18 Graph of projectile velocity from test and calculations 45
- Figure 19 Local deformation in wall 52
- Figure 20 Area under stress-strain curve..... 53
- Figure 21 Perforation thin steel plate 54
- Figure 22 Reinforced concrete 57
- Figure 23 Fiber-reinforced concrete 60
- Figure 24 Model of the testing area..... 61
- Figure 25 Existing safety walls 65
- Figure 26 Scabbing of safety wall 68
- Figure 27 Moment forces existing safety walls..... 69
- Figure 28 Steel barrier 70
- Figure 29 Cross-section of frame 72
- Figure 30 Analysis of deflection of steel wall..... 73
- Figure 31 Shear forces..... 75
- Figure 32 Composite safety walls with bolted steel plate 76
- Figure 33 Existing safety walls with welded plate 77
- Figure 34 New testing area with existing safety walls 80

Table list

Table 1 Risk acceptance criteria.....	9
Table 2 Probability scale	10
Table 3 Severity scale.....	10
Table 4 Risk rating scale	11
Table 5 Distribution of energy in a failure	14
Table 6 Fundamental penetration formulas	26
Table 7 Range of empirical formulas for calculating penetration of concrete	29
Table 8 Results preliminary calculations M3-Pins.....	39
Table 9 Ultimate tensile strength vs Ultimate shear strength.....	39
Table 10 Results of preliminary calculations Baker equation.....	41
Table 11 Preliminary calculation results based on first law of thermodynamics.....	41
Table 12 Preliminary trajectory results	42
Table 13 Test results.....	44
Table 14 Comparison of test results and calculations	44
Table 15 The 200 bar FAT-test of a 48" Smartplug.....	47
Table 16 Properties of 500 bar structural test Smartlay	48
Table 17 Result of pressure wave.....	49
Table 18 Water jet results.....	49
Table 19 Steel properties	54
Table 20 Properties of fixed safety walls	62
Table 21 Properties of small projectiles	62
Table 22 Penetration results of fixed safety walls.....	63
Table 23 Penetration depth on fixed safety walls from the analytical model	63
Table 24 Penetration depth with high strength concrete	63
Table 25 Perforation results from empirical formulas for fixed safety walls.....	64
Table 26 Perforation thickness for fixed safety walls	64
Table 27 Properties of existing safety walls.....	66
Table 28 Penetration results of existing safety walls	66
Table 29 Penetration depth of existing safety walls based on analytic model.....	66
Table 30 Perforation results existing safety walls.....	67
Table 31 Perforation thickness existing safety walls	67
Table 32 Properties of large projectiles.....	69
Table 33 Energy absorption with wall thickness 0.02 m.....	71
Table 34 Energy absorption with wall thickness 0.025 m.....	71
Table 35 Frame properties for steel wall.....	72
Table 36 Forces acting on wall.....	72
Table 37 Properties wall.....	73

Table 38 Steel walls resistance to shear force	74
Table 39 Force from large projectiles	74

Abbreviations or List of symbols. Probably the last.

Explain the words (NDRC, TNT, Etc)

1 Introduction

1.1 Background

During pressure testing using pressurized vessels on a workshop floor, the surrounding areas needs protection. This is due to the possibility of test failure. A result of failure could be high-pressure water jet or discharge of a projectile. *Figure 1* illustrate two plug models inside a pipe. A permanent shield may provide the protection as part of the test bay design, but it is necessary with access to the testing area to setup and operate the pressure test. The installation and removal of test vessels is done by crane or forklift so part of the shield should of practical reasons be made portable. The safety walls should be made of reinforced concrete blocks or section of walls. The walls and blocks have limitations to width, height and weight since they should be portable by crane or forklift.

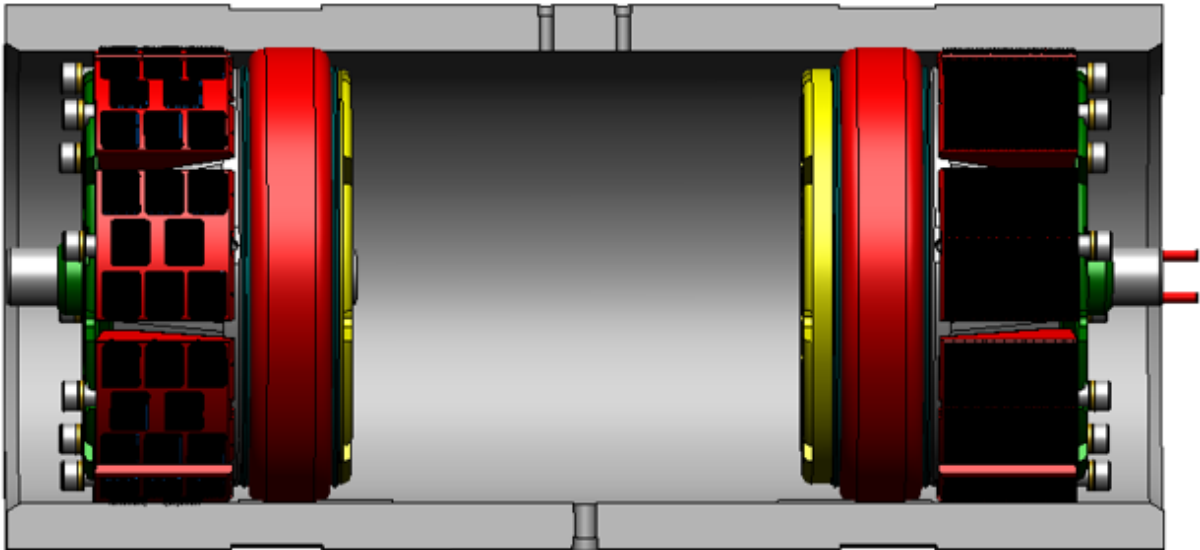


Figure 1 Model of two plugs inside the pipe

1.2 Objective

There are no previous calculations done regarding the safety installments already in place, however the thesis will analyze the forces and risks involved in case of failure. Further, the thesis will decide if the walls are sufficient as protection. Based on the results from calculation and testing, the thesis will develop a design of safety walls to provide necessary protection during pressure testing. The wall is required to provide a suitable and acceptable protection against potential incidents. The thesis will also investigate if the walls are damaged beyond repair or reusable in case of failure. If the wall is insufficient as protection, the thesis should provide other mediating alternatives.

1.3 *Scope of work*

The thesis will involve study of codes and regulations regarding hydrostatic pressure testing. This involves mostly theory on hydro testing of pipelines. The thesis focuses on hydrostatic pressure due to safety regulations at TDW. Further, it is necessary to calculate and determine the potential energy in a pressurized vessel and effects of failure. One of the main issues is how much of the potential energy is transferred into kinetic energy in a failure. Based on these calculations, design of barriers is discussed to fulfill safety requirements of the testing area. The final design should be within reasonable price range and have maximum weight and size criteria. The walls should be easily portable as they are relocated between each test.

2 Safety Requirements during Pressure testing

The regulation on pressure testing in Norway categorizes high pressure as more than 0,5 bar. Accordingly, equipment with allowable maximum pressure above 0,5 bar, should be made according to regulation on compressive loads and be CE-approved.

The regulations in Norway that cover safety during safety testing is quite wide and gives no specific requirements to the safety level. According to Forskrift om håndtering av farlig stoff (2009) (Regulation on Managing Dangerous Matter), §14 states that a risk analysis should be conducted for the pressure test. This implies identification of hazards and the owner and operator should lower the risk to a reasonable level. According to *Forskrift om trykkpåkjent utstyr (1999)* (Regulation regarding Pressure-Loaded Equipment), Vedlegg 1 Innledende krav (Appendix 1 Preliminary requirements) states that the risk should be eliminated or reduced to a reasonable level. There should be a suitable protective measure to diminish the risk that could not be eliminated. The user of the area should be informed about the remaining risk.

A risk analysis is a tool for documenting how to achieve a reasonable security level. A thorough risk analysis should include risk as a product of probability and severity as well as expand for mitigating actions and determine remaining risk. The analysis should also include internal and external circumstances as well as undesirable elements. Based on the analysis, sufficient measures should be implemented to reduce the risk to an acceptable level. To make a complete risk analysis for the desired area or operation, several different people or departments should be involved in the process. This is to easier identify and find suitable mitigation actions against possible hazards. The company is also required to review and update the risk analysis regularly.

When constructing a new facility, or when altering an existing facility, it is necessary to perform a risk analysis in advance. The analysis should include undesirable incidents and its consequences towards life, health, environment and material values. For existing facilities, it is necessary to do a systematic mapping of dangers and undesirable incidents.

3 Energy stored in pressurized vessel

Pressure is compression of volume by the use of energy. If a failure occurs, this energy is released at a high rate. The definition of pressure is force divided by area (*Eq. 3.1*). The relation illustrates that the force can change based on both area and pressure. Still, a large area with low pressure can have the same amount of energy as a small area with high pressure.

$$P = \frac{F}{A} \quad \text{Eq. 3.1}$$

Where P is the pressure, F is force and A is the cross-sectional area. Energy is measured as a product of force and the distance it moved, or in this case, as a product of pressure and change in volume. Due to its high compressibility, gas is considered a great hazard.

Energy in a vessel could also be estimated by pressure as a product of change in volume in addition to temperature as a product of change in entropy. The first law of thermodynamics (*Eq. 3.2*) defines change in energy as:

$$dU = dQ - dW = TdS - PdV \quad \text{Eq. 3.2}$$

Here U is the total energy in the vessel, Q the heat energy and W the work performed due to the pressure. Further, T is the temperature of the test medium, S is the entropy of the medium and V is the volume of the medium. Here it is important to include the expansion of the test vessel due to the pressure, as this also alters the volume. This is considered as work energy.

This thesis will focus on the events from hydro-pressure. Since water has low compressibility especially compared to gas, the energy stored in a pressurized vessel is lower. Still, when operating with high pressure or large volumes, a sudden burst of energy can cause a hazardous situation. The main hazards in a failure during pressure testing are a pressure wave, water jet, burst of water hose, fragments and projectile discharge as well as ejection of a plug. The thesis will through calculation and a risk analysis assess these hazards and give suggestions to mitigating measures.

4 Risk analysis

Risk is a term to describe danger or hazards in daily life. The level of risk is usually decided by both the frequency of an incident and its severity as shown in *Eq. 4.1*.

$$\text{Risk} = \text{Frequency} \cdot \text{Severity} \qquad \text{Eq. 4.1}$$

What determines the level of risk is the frequency of an incident and the consequence for when that incident occurs. The frequency is determined by statistical data. With the lack of statistics, a subjective estimation of a reasonable probability is required. The severity is determined by an assessment of the operation and identification of hazards. In the assessment, it is necessary to include every scenario that might happen. For a better understanding of risk and the elements of a risk analysis, a better definition of risk is necessary.

4.1 Risk

The objective of a risk analysis is to describe and reduce risk. To achieve a better understanding of the risk analysis, it is necessary to thoroughly define risk and how it is expressed. Risk is related to a future event and their outcomes. There is uncertainty related to both the future events and their outcomes. In other words, the uncertainty of a future event to occur and with that a specific outcome will happen. The result can be referred to as the probability of an outcome based on background knowledge. It is important to separate between uncertainty and probability because probability is a tool to describe uncertainty between the event and an outcome. Uncertainties might be hidden in background knowledge. An example is a structure with probability of failures with the assumption that the structure will be able to handle a certain accidental load. In real life, the structure might fail at lower load level because of uncertainty in the material strength, model geometry, construction and so on.

Each element will be given an uncertainty, and if this value is high, the factor is given a high risk score. To obtain a high score, the factor must be considered as important for the risk aspects considered as well as a large uncertainty.

4.2 *Description of risk*

There are different ways to describe risk. A commonly used term is the *Fatality Accident Rate* (FAR). The FAR describes the level of risk regarding loss of lives. The expected number of fatalities for each 100 million workhours decides the FAR value. To describe fatalities per year the *Potential Loss of Life* (PLL) is used. Due to lack of data concerning failures and failure rate in pressure testing, this thesis uses the safety functions model. Risk associated with loss of safety functions is the result of change in probability or frequency due to impairment of the safety function. The risk analysis gives an assessment of the risk with and without the safety functions. The main safety functions to consider during pressure testing is based on *PSA* (2001):

- Protect rooms of significance.
- Protect safe areas
- Maintain at least one evacuation route from every manned area.

How well these areas should be protected is reviewed later in the thesis.

4.3 *Severity, Probability and uncertainty*

The determination of the severity for each initiating event is an important part of risk analysis. Here all the damages and injuries from the possible events are considered. In this thesis, the severity will be based on loss of life or injury to personnel. Other common categories are financial loss, environmental damage and loss of reputation. The different categories are linked to some degree, however different types of events give different type of consequence. For instance, frequent small accidents may tarnish the reputation more than any other category.

An Event tree is frequently used to categorize and separate these different types of losses in an organized way. An event tree shows all the initiating events and all the steps and events necessary for the safety barriers. A safety barrier is a mitigating action to prevent injury or damage during a failure. The aim of the barriers is to reduce the outcomes to an acceptable level. For each event, it is possible to perform a barrier analysis to study the effect of failure by the barriers.

The *Figure 2* shows the event of a *Pipe rupture*. The first barrier is *Safety walls*. If the *Safety walls* prevent the danger, it is considered a success and it is not necessary with the next barrier. If the walls are perforated and reduce the hazard, it is considered a *Partly success*. However, if the hazard misses the safety walls, it is considered as ineffective. The next barrier is the barrier *Safety area*. This is a closed off area behind the safety walls. The *Outcome* explains the severity for each case, which is numbered after the degree of consequence. The numbering of the events is not related to any value of actual consequence, but is categorized according to possible damage.

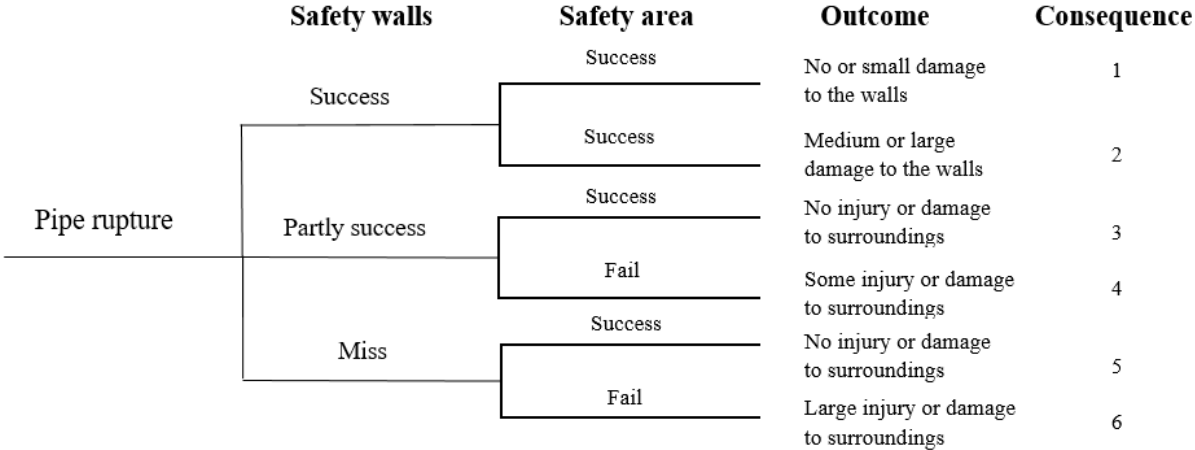


Figure 2 Event tree of pipe rupture

By doing a consequence analysis to assess the severity of an event, it is important to understand the physical phenomena of the incident. As this thesis focuses on hazards regarding hydro testing of pipelines, the first thing to consider is the potential forces in a pressure test. Further, it is necessary to identify and evaluate each of the hazards in terms of severity.

To determine how likely a hazard is to happen, it is necessary to determine the probability of the event. The probability is based on background knowledge, but does not account for possible lack of information. With this in mind, it is necessary to introduce uncertainty in the equation. To do this means to be conservative.

4.4 Hazard

A hazard is any form of potential harm, damage and health effects under certain conditions. From the stored energy in a pressurized vessel, there are five main hazards in relation to a failure.

The most critical hazard is if the plug or end section of pipe is released. The cross-sectional area of both the plug and the end section is quite large, so from the relation with pressure and contact area there are great forces at play. The amount of energy in a discharge is based on compressibility of the test medium and contraction of the vessel. As stated earlier, gas volume will expand multiple times the volume of a liquid depending on the pressure. This indicates that the energy transferred to a plug or end section will be considerable larger in a failure involving a gas medium than a liquid.

Another hazard is ejection of fragments from the pipe. In this case, the fragments are considered to have low mass and high velocity. They will hereby be referred to as projectiles. The same relation between compressibility and energy release as above applies for this case as well. The size, shape and weight of a projectile is difficult to determine as it is uncertain which section of the pipe or plug that could be ejected.

The third hazard is a water jet from a leak. The velocity of this jet will be quite high, but the volume released will be low. This is because water is not easily compressed. This will result in water pressure dissipating quickly after release. A gas jet is of much larger consequence due to temperature change or toxic fumes. The vessel will discharge large quantities of gas during a failure and can create a hostile environment. Another hazard concerning a jet discharge is a two-phase jet. Gas is compressed into liquid form due to pressure or temperature, but when ejected from the vessel, the test medium is returned to gas. This results in massive volume change and hot gas can cause major harm. For example, hot water will turn into steam, which will scold people who makes contact.

A fourth hazard is a pressure wave created from sudden change in volume. An impulsive change in volume will create a pressure wave, which would diminish over a distance. To calculate the safe distance in case of such a wave, the energy is converted into grams of Trinitrotoulen (TNT). With different parameters, it is possible to determine a safe distance.

The last hazard is the burst of a pressure nozzle with connected hose. The hose will start flying around and act as a whip. The pressure nozzle at the end of the hose could cause serious injury and damage to nearby personnel and equipment. *Figure 3* shows a similar situation where the pressure is not bled out, and the valve is released. The valve is released as a projectile towards the operator. This is one of the more common hazards to happen during pressure testing. *Figure 3* is an illustration of an incident which led to a fatality in BC, Canada.

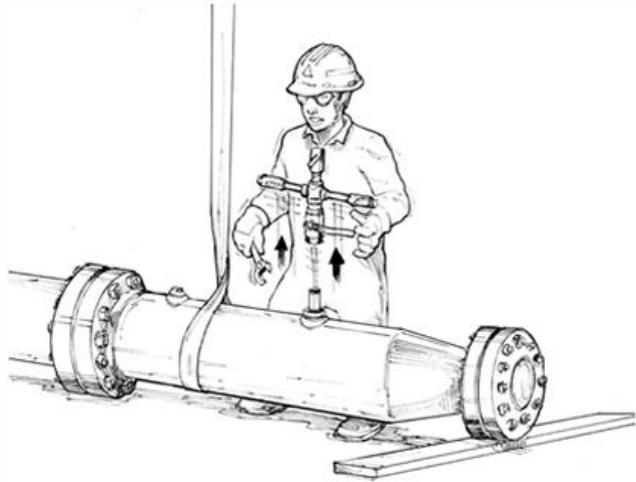


Figure 3 Operator removes a valve under pressure

4.5 Risk acceptance criteria

When the calculated risk is lower than the appointed risk, the measures are sufficient and the risk is acceptable. For instance, if the frequency of an incident which impairs a safety function exceeds the limit, the risk is unacceptable. The appointed risk is often determined by a risk scale matrix. The *table 1* shows a risk scale matrix from TDW, which is the basis for this thesis’s risk acceptance criteria. The next tables show the probability scale, severity scale and Risk rating scale to explain the different levels of risk. To achieve risk acceptance criteria, it is necessary to treat risk. First, it is necessary to assess what is acceptable and how to achieve this level of risk.

Table 1 Risk acceptance criteria

		Severity S				
		1	2	3	4	5
Probability P	5	5	10	15	20	25
	4	4	8	12	16	20
	3	3	6	9	12	15
	2	2	4	6	8	10
	1	1	2	3	4	5

The larger scale or more levels a risk matrix have, the more accurate it can describe the risk. The usual size is between a 4-level and a 6-level matrix. The colors are a visual aid to determine the scale of acceptance. The colors are explained later in this chapter. *Appendix A* shows the risk analysis, which the thesis is based on. The hazards are appointed probability and severity values to determine if the risk is acceptable.

To determine a value in the risk acceptance scale, it is necessary to determine the probability and severity. *Table 2* and *Table 3* show the definition and explanation of each number in the scale. The explanations and definitions inside the tables should be based on FAR or PLL values. Thus, to get a better understanding of the risk picture and to properly assign the risk acceptance criteria.

Table 2 Probability scale

P		Probability of Occurrence
1	Improbable	Very rare occurrence. Can occur only in exceptional circumstances. Requires sequential / multiple system failures for event occurrence.
2	Remote	Less likely. Can occur remotely in 5 years (once or twice)
3	Occasional	May be possible. Occurs once / twice in a year
4	Probable	Likely occurrence. Occurs few times in a month. Can be consistent week after week.
5	Frequent	High probability. Occurs very frequently, many times in a working day / week. Highly certain, constant and continuous exposure exists

Table 3 Severity scale

S		Harm to Personnel (Health & Safety)
1	Negligible	First Aid incident
2	Marginal	Medical Treatment Only / Minor health effects like skin irritation, eye irritation, etc.
3	Critical	Up to a Restricted Work Case / Reversible Health Effects affecting normal work activity
4	Severe	Up to a Lost Time Injury / Reversible Health Effects requiring days of work off
5	Catastrophic	Fatality, multiple severe or critical injuries / Irreversible Health Effects (Eg. Compensable Diseases as per Local Laws)

Table 4 gives a description to each of the colors in the risk acceptance scale. Each color has a level of security to easily categorize the risk in an operation.

Table 4 Risk rating scale

R	Harm to Personnel (Health & Safety)
Low-Level 4 (1 - 4)	Activities in this category contain minimal risk and are unlikely to occur. Organizations can proceed with these activities as planned.
Medium-Level 3 (5 - 9)	Contains some level of risk that may occur. Facilities should consider what can be done to manage the risk to prevent any negative outcomes.
High-Level 2 (10 - 14)	Contains potentially serious risks that are likely to occur. Application of proactive risk management strategies to reduce the risk is advised. Facilities should consider ways to modify or eliminate unacceptable risks.
Extreme High Level 1 (15 - 25)	Contains unacceptable levels of risk, including catastrophic and severe injuries and / or health risk that are most frequently to occur. Facilities should consider whether they should eliminate or modify activities that still have Level 1 rating after applying all reasonable risk management strategies

4.6 ALARP

ALARP or *As Low As Reasonable Practicable* is a popular tool when treating risk. For every operation, the ideal would be to have no risk. Unfortunately, this is not possible. Therefore the risk should be reduced to a reasonable level. ALARP was developed to assess measures in terms of disadvantages and cost. The assessment is done to compare the cost and disadvantages of a measure with the benefits. To determine the difference, it is necessary with a crude analysis of the pros and cons of the different alternatives. The analysis should be qualitative and the results illustrated through a matrix with four to six levels.

An additional analysis will provide a better basis for which alternative to select. This may include risk analysis, cost analysis and analysis to show the degree of sufficiency. Further, it is necessary to perform an assessment of uncertainties and events. This assessment determines if it is necessary with a more thorough analysis.

In the end a total evaluation of the different analyses should be performed. The discussion of the results with regard to limitations of the analysis should also be included. This thesis will not do a cost analysis as it is outside of the scope, but will by a risk analysis and calculations determine if the alternatives are sufficient and give recommendations for improvement. The alternatives will be assessed in terms of cost, but only as an estimate.

5 Assessment of hazards through calculations

The potential energy in a pressurized vessel could be calculated in different ways. To calculate the energy through thermodynamics the first law of thermodynamics (*Eq. 3.2*) is necessary. This relation involves the energy from the compression of the liquid and expansion due to different heat energy through integration. According to Manning (2005) the heat term is usually neglected during hydrostatic pressure.

The force acting on a projectile, plug or end section is given by *Eq. 3.1*. Further, the potential energy is determined by the pressure as a product of the change in volume due to compression.

Eq. 5.1 from Baker (1973) is called the Baker formula. The formula calculates the potential energy in a vessel based on the relation between pressure, volume and bulk modulus of the liquid.

$$U_w = \frac{1}{2} \cdot \frac{1}{\beta} \cdot P^2 \cdot V = \frac{1}{2} \cdot C \cdot P^2 \cdot V \quad \text{Eq. 5.1}$$

Where U_w is the energy in the compressed liquid, β is the bulk modulus and C is the compressibility of the liquid. This formula shows that the potential energy changes linearly with the volume and quadratic with the pressure. The compressibility of the fluid will change depending on the pressure, but for the calculations in this thesis the value is a conservative constant.

The pipe will expand due to high pressure. To calculate the expansion in the pipe the equation is based either on the strain calculations through stress in the pipe or on a direct calculation through the elasticity modulus. If the pipe bursts, the elastic energy in the pipe will be released as a sudden change in volume. To calculate this, it is necessary to know the specifications of the pipe. To calculate the strain through the stress of the pipe, it is essential to calculate hoop and longitudinal stress. The calculations of hoop and longitudinal stress for a thin walled pipe based on Fenner and Reddy (1999) is given by *Eq. 5.2* and *Eq. 5.3*, respectively.

$$\sigma_H = \frac{P \cdot D}{2 \cdot t} \quad \text{Eq. 5.2}$$

$$\sigma_L = \frac{P \cdot D}{4 \cdot t} \quad \text{Eq. 5.3}$$

Where σ_H is hoop stress, D is the inner diameter, σ_L is the longitudinal stress and t is the wall thickness of the pipe. The wall thickness of a thin-walled pipe is categorized as less 1/10 of the diameter. For tests with larger pressure, this is usually not the case.

Hoop and longitudinal stress is given by Eq. 5.4 and Eq. 5.5 for a thick-walled pipe, respectively.

$$\sigma_H = \frac{P \cdot D_i^2}{D_o^2 - D_i^2} + \frac{D_o^2 \cdot P}{D_o^2 - D_i^2} = P \frac{D_i^2 + D_o^2}{D_o^2 - D_i^2} \quad \text{Eq. 5.4}$$

$$\sigma_L = \frac{P \cdot D_i^2}{D_o^2 - D_i^2} \quad \text{Eq. 5.5}$$

Here D_i is the inner diameter and D_o is the outer diameter of the pipe.

Next step is to calculate the strain (Eq. 5.6 and Eq. 5.7) from both hoop stress (Eq. 5.2 or Eq. 5.4) and longitudinal stress (Eq. 5.3 or Eq. 5.5).

$$\epsilon_H = \frac{\sigma_H}{E} - \frac{\sigma_L \cdot \nu}{E} \quad \text{Eq. 5.6}$$

$$\epsilon_L = \frac{\sigma_L}{E} - \frac{\sigma_H \cdot \nu}{E} \quad \text{Eq. 5.7}$$

Here is ϵ_H hoop strain, E is the young's modulus, ν is the Poisson ratio and ϵ_L is the longitudinal strain. Figure 4 illustrates how pressure works and give direction to the stress acting on the pipe.

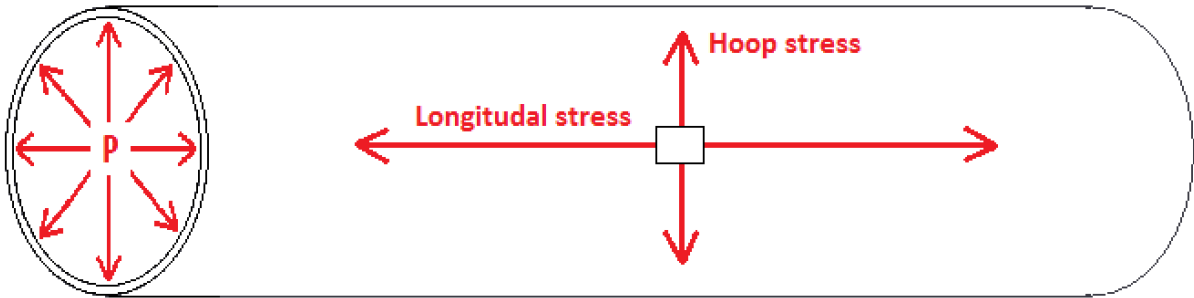


Figure 4 Hoop stress and longitudinal stress in a pipe

By calculating the final volume (Eq. 5.8) while the pipe is experiencing strain, it is possibility to find the change in volume (Eq. 5.9).

$$V_f = \frac{\pi}{4} \cdot [D \cdot (1 + \epsilon_H)]^2 \cdot [L \cdot (1 + \epsilon_L)] \quad \text{Eq. 5.8}$$

$$\Delta V_m = V_f - V \quad \text{Eq. 5.9}$$

Where V_f is the final volume, L is the pipe length and ΔV_m the expansion due to strain. The elastic energy stored from the strain in the pipe is given by Eq. 5.10.

$$U_m = 0.5 \cdot P \cdot \Delta V_m \quad \text{Eq. 5.10}$$

Here U_m is the elastic energy in the material.

According to Manning (2005) the elastic energy stored in the pipe can also be expressed by Eq. 5.11.

$$U_m = \frac{P^2 \cdot V}{2 \cdot E} \cdot \left[\frac{3 \cdot (1 - 2 \cdot \nu) + 2 \cdot \delta^2 \cdot (1 + \nu)}{\delta^2 - 1} \right] \quad \text{Eq. 5.11}$$

Where δ is the diameter ratio. Eq. 5.11 gives less energy release than the calculations with strain of the pipe. It also neglects elastic deformation in the ends. The elastic pipe energy together with the potential energy in compressed water can give a total energy burst given in Eq. 5.12.

$$U_T = U_w + U_m \quad \text{Eq. 5.12}$$

From the previous formulas, it is possible to determine the potential energy in a pressurized vessel. However, how much of this energy is transmitted into each of the hazards is yet to be determined. Other factors that determine the potential energy might be air bobbles inside the vessel, temperature change during the test in both the material and liquid, uncertainties in the measuring devices and inaccurate formulas.

The amount of energy that is directed to each of the hazards is uncertain. According to Cox & Saville (1975) the energy distribution in the event of a total collapse of pipe is shown by Table 5. The values have been tested to some degree, but only in terms of kinetic energy.

Table 5 Distribution of energy in a failure

	Shock wave energy	Fragment kinetic energy
<i>Complete shattering of vessel due to brittle failure</i>	$0.8 U_T$	$0.2 U_T$
<i>Ejection of a major vessel section such as an end closure of a short, large bore vessel</i>	$0.4 U_T$	$0.6 U_T$

Figure 5 shows different scenarios of failure of the pipe. Complete rupture of vessel (left), breaking into two due to rupture (middle) and fragmentation (right)

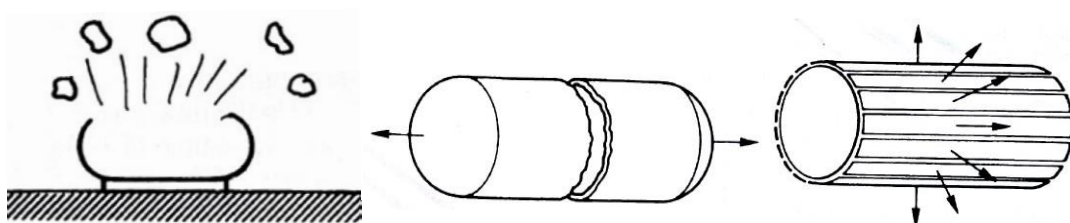


Figure 5 Different scenarios of failure of a pipe

5.1 Pressure wave

One of the hazards that will always occur if there is a burst of energy is a pressure wave. The energy and level of danger of this hazard is based on speed and the amount of energy which is released from the pipe. A pressure wave, if large enough, could have a devastating effect. For instance, a small wave could rupture an eardrum while a larger wave will crush internal organs and may lead to a fatality. *Figure 6* is an illustration of a shock wave without any obstacles.

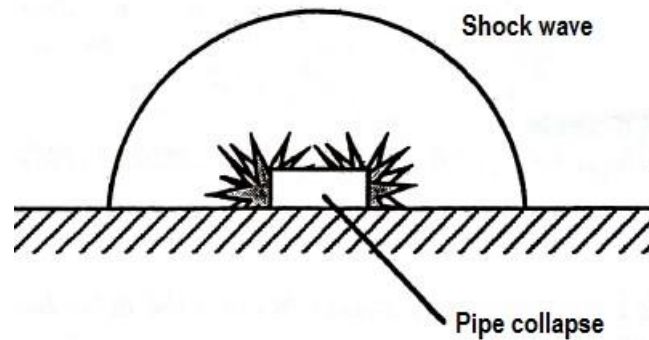


Figure 6 Pipe collapse with shock wave

To determine a safe zone from the pressure wave, Kinney and Graham (1985) found the relation between rapid energy release and the explosive energy of TNT. The energy is therefore transformed into weight of TNT. How similar a pipe burst is to a detonation of TNT is uncertain, but this is the best way to describe a sudden energy release. *Eq. 5.13* converts the energy into grams of TNT.

$$W_{TNT} = \frac{E}{4.850 \cdot 10^3} \quad \text{Eq. 5.13}$$

Where W_{TNT} is the weight of TNT in [g] for each [joule] of energy. Further, the safe distance from the energy center is expressed by *Eq. 5.14*.

$$R = k \cdot W^n \quad \text{Eq. 5.14}$$

Here R is the distance from the energy center while k and n are constants to determine the safety class. This distance is when there is no obstacles inside Paulsen (2009) defines the safe distance as $k = 6$ [m] and $n = 1/3$. To find the distance to which there is a risk of eardrum rupture the k -value is changed to 0.45 [m].

These results are for when there are no obstacles to the pressure wave. The safe distance is also given with a conservative parameter. From the pressure tests with liquid that are conducted at TDW, the pressure wave will have close to no effect on the surrounding structure and safety walls.

5.2 Water jet

A water jet is a rapid discharge of water due to high pressure. The dangers to personnel related to a water jet is cuts and internal damages. *Figure 7* shows how the water jet acts during a projectile discharge.



Figure 7 Water jet during projectile test

To calculate the velocity of a water jet, the use of *Bernoulli's formula* is essential (Eq. 5.15).

$$\frac{1}{\rho}(P_1 - P_2) + g(z_1 - z_2) = \Delta\left(\frac{u^2}{2}\right) + F_F \quad \text{Eq. 5.15}$$

Here ρ is the density of the fluid, P_1 and P_2 is the pressure inside and outside of the vessel and g is the gravitational acceleration. z_1 and z_2 are the heights at the discharge compared to the top of the pipe, Δu is the change of velocity in the water and F_F is friction force. The variation in elevation is of small importance when working with the high pressure so this section is

usually neglected. To calculate the change in velocity from stationary to discharge, it is necessary to solve Eq. 5.15 with respect to Δu (Eq. 5.16).

$$\Delta u = \sqrt{2 \cdot \left[\frac{1}{\rho} (P_1 - P_2) + g(z_1 - z_2) - F_F \right]} \quad \text{Eq. 5.16}$$

Eq. 5.17 and Eq. 5.18 are for calculation of water discharge in a large manner. When estimating the frictional loss F_F , there is frictional loss due to sudden contraction, due to pipe friction and frictional loss due to fittings. Expansion losses have been ignored, as they cannot exceed the kinetic energy of the fluid and do not apply at the point of discharge to the atmosphere. The friction loss from contraction is given as Eq. 5.17.

$$F_c = 0.4 \left(1 - \frac{A_2}{A_1} \right) \left(\frac{u^2}{2} \right) \quad \text{Eq. 5.17}$$

Here F_c is the friction loss from contraction while A_2 and A_1 is the change of area in the pipe. This formula uses the change in area as basis. For our case, this will be the elastic contraction of the pressurized pipe after pressure release. The friction loss from the pipe is given as Eq. 5.18.

$$F_f = \frac{4fl}{D} \left(\frac{u^2}{2} \right) \quad \text{Eq. 5.18}$$

Where F_f is the friction loss from the pipe, f is the friction coefficient, l is the length of the pipe and D is the diameter of the pipe.

5.2.1 Liquid discharge rates through a small orifice

This section focuses more on liquid discharge through an orifice. The orifice is defined as small compared to the vessel. *Eq. 5.19* calculates a general size of a leak based on SINTEF (2003).

$$A = 0.475 \cdot R \cdot t \quad \text{Eq. 5.19}$$

Eq. 5.19 depends on the radius of the pipe R and thickness of the pipe wall t and A is the cross-sectional area of the leak. *Eq. 5.20* for discharge through this orifice or leak, neglects changes in elevation and there are less frictional losses than the flow kinetic energy.

$$u = C_D \sqrt{\left[\frac{2}{\rho} (P_1 - P_2) \right]} \quad \text{Eq. 5.20}$$

This can also be expressed in terms of mass rate W in *Eq. 5.21*.

$$W = C_D \cdot A \sqrt{[2\rho (P_1 - P_2)]} \quad \text{Eq. 5.21}$$

C_D is the coefficient for a theoretical discharge. The actual discharge is the product of the actual cross-sectional area and velocity of the jet. According to Lewitt (1952) and Coulson and Richardson (1977-) the limiting values of the coefficient C_D are 0.6 and 0.85 at high and low-pressure ratios, respectively.

5.2.2 Dispersion of Jet

The path of a liquid jet can be quite large. It may reach beyond the limit of the area classification zone. The simplest way to think of a liquid jet is that it suffers no drag or dispersion. For a jet at ground level, the motion in the horizontal direction is defined by *Eq. 5.22*.

$$\frac{dx}{dt} = u \cdot \cos \alpha \quad \text{Eq. 5.22}$$

Where t is the time from release to touch down point (TDP), x is the horizontal distance to TDP and α is the angle of the jet in relation to the horizontal. The next derivations are under *Appendix B*.

The maximum distance of travel x_{max} occurs at $\alpha = 45^\circ$ (*Eq. 5.23*).

$$x_{max} = \frac{u^2}{2g} \quad \text{Eq. 5.23}$$

For an elevated jet, the jet returns to the ground at $t = t, z = -z$ and, by calculating in the same approach, the distance is given by *Eq. 5.24*, where z is the height above ground.

$$x = \frac{u^2}{g} \left\{ \frac{\sin 2\alpha}{2} + \sqrt{\left[\left(\frac{\sin 2\alpha}{2} \right)^2 + \frac{2l \cdot g \cdot \cos 2\alpha}{u^2} \right]} \right\} \quad \text{Eq. 5.24}$$

For a horizontal elevated jet, the following simple treatment is applicable (Eq. 5.25 and Eq. 5.26).

$$x = ut \quad \text{Eq. 5.25}$$

$$z = \frac{1}{2}gt^2 \quad \text{Eq. 5.26}$$

From Eq. 5.25 and Eq. 5.26 we get the distance expressed by Eq. 5.27.

$$x = u \left(\frac{2z}{g} \right)^{1/2} \quad \text{Eq. 5.27}$$

In actual situations, the travel distance of a liquid jet will be less than what the equations above predict. The jet is subjected to air resistance and to disintegration. A usual assumption is that the actual travel distance of the jet is halved due to dimidiation by drag force and disintegration Manning (2005). As the volume of water discharged is small, the damage the water jet could do to the safety walls is minimal. The danger associated with this hazard is if personnel is close to the pipe at the time of discharge. Examples of injuries is if the pressure is not bled out, and someone open a valve under pressure.

5.3 Small, high velocity projectiles

Due to the stored energy or a rupture, the release of fragments is a possibility. Since there is large amount of energy and the fragments usually have low mass, these fragments will have large velocity. That makes projectiles a dangerous hazard, and manned areas should have barrier protection to prevent damage. Figure 8 shows the projectile used during testing of discharge.



Figure 8 Projectile used during testing

To calculate the kinetic energy of a fragment the total energy during a burst is necessary (Eq. 5.28).

$$E_k = \frac{1}{2} \cdot m \cdot v^2 \quad \text{Eq. 5.28}$$

Where E_k is kinetic energy of object, m is the mass and v is the velocity of the object. As we can determine the kinetic energy, it is possible to find the fragments velocity (Eq. 5.29) through a transformation of Eq. 5.28.

$$v = \sqrt{2 \cdot \frac{E_k}{m_{Proj}}} \quad \text{Eq. 5.29}$$

Where m_{Proj} is the mass of the discharged projectile. This will give quite large velocity for small projectiles. Eq. 5.29 is based on one projectile. To account for multiple projectiles it is necessary to use the total mass, but it might not give an exact value.

The trajectory of the fragment depends on the angle of discharge. The distance of the fragment is calculated by Eq. 5.24.

This equation does not take air resistance or any obstacles into account, which makes it a conservative calculation. The main reason is that the air resistance is a function of the shape and velocity, which is unknown.

5.4 Plug discharge

One of the most dangerous hazards is the release of a plug or the end of the pipe. It has a large cross-section area compared to the size of the pipe. The easiest way to calculate the force acting on the plug is to look at the force-pressure relation (Eq. 3.2).

To calculate the theoretical energy a plug will have in a discharge, the pressure is multiplied by the change in volume. Both the elastic expansion of the pipe (Eq. 5.30) and the compression of water (Eq. 5.31) are factors affecting the volume.

$$E_{plug} = \Delta V_{total} \cdot P \quad \text{Eq. 5.30}$$

$$\Delta V_{total} = \Delta V_m + \Delta V_w \quad \text{Eq. 5.31}$$

Here E_{plug} is the kinetic energy of the plug, ΔV_{total} is the combined change in volume from elastic strain in the pipe ΔV_m and compressed water ΔV_w . This theoretical method implies that all energy is transformed into kinetic energy. In case of a discharge energy will go to friction force and to release the plug. According to Table 5, the energy transformed into kinetic energy of the plug or the end of the pipe is Eq. 5.32.

$$E_k = 0.6 \cdot E_{plug} \quad \text{Eq. 5.32}$$

To calculate the change in volume for the compressed water it is necessary to use thermodynamics and the specific volume. By using *Appendix B* for water, it is possible to calculate the initial volume (*Eq. 5.33*) and final volume (*Eq. 5.34*).

$$V_i = v_i \cdot m \quad \text{Eq. 5.33}$$

$$V_f = v_f \cdot m \quad \text{Eq. 5.34}$$

Where V_i is the initial volume of water, v_i is the specific volume of water in atmospheric pressure ($0.001 \text{ m}^3/\text{kg}$) and m is the mass of the water inside the vessel. Further, V_f is the final volume of water and v_f is the specific volume of water under pressure.

The work performed to compress the water can be calculated by *Eq. 5.35* and change in volume is expressed by *Eq. 5.36*.

$$W = \int_{V_i}^{V_f} P dV = \Delta V_w \cdot P \quad \text{Eq. 5.35}$$

$$\Delta V_w = V_f - V_i \quad \text{Eq. 5.36}$$

Here is W the work necessary to compress the water. This is a complete theoretical calculation and many parameters will affect the result.

Another way to calculate the velocity of the plug (*Eq. 5.37*) is to use the *Eq. 5.29*.

$$v = \sqrt{2 \cdot \frac{E_k}{m_{plug}}} \quad \text{Eq. 5.37}$$

Where v is the plug velocity and m_{plug} is the weight of the plug.

6 Safety walls theory

In case of a failure in a pipe, it is probable that a discharged projectile might cause injury. To prevent this, safety walls are erected around the test vessel. The walls should be able to reduce the risk to an acceptable level. To do this, the walls have to reduce or stop the energy from a hazard. The hazards considered in the thesis are pressure wave, fragment, water jet, bursting hose, plug module and end section of a pipe.

All hazards except the pressure wave are considered as kinetic energy. Therefore, these will have a direct impact on the walls. A water jet will dissipate quickly as there are small amounts of water in the stream. A discharge of a fragment, plug module and end section of the pipe will have large amounts of kinetic energy. They are therefor basis for calculating the walls. The calculations on penetration and perforation on the walls are based on empirical formulas.

6.1 Impulse force

To design a wall, it is necessary to calculate the force in an impact. Impulse force is considered as objects with large magnitude, which act over a very small time interval, but cause a significant change in the momentum. A high velocity projectile will have large impulse force due to rapid negative acceleration. The rate of which an object decelerate, is determined by the deformation in both the object and the target. Another factor is the time interval of the deformation. To appoint these values accurately it is necessary to conduct impact tests for the desired materials. For a steel ball, bouncing on a steel plate, the typical time interval is approximately 0.0002 seconds. However, this is of course dependent on the initial velocity and the size of the deformation.

From Newton's second law we have *Eq. 6.1*.

$$F = m \cdot a = m \cdot \frac{dv}{dt} = \frac{d}{dt}(m \cdot v) \quad \text{Eq. 6.1}$$

Where F , m , a and v is force, mass, acceleration and velocity of the projectile, respectively. To define the impulse force of the impact (*Eq. 6.2*) it is necessary to integrate between the time interval of the impact.

$$\int_{t_1}^{t_2} F dt = F(t_2 - t_1) = \Delta(m \cdot v) \quad \text{Eq. 6.2}$$

Eq. 6.2 gives Eq. 6.3:

$$F = \frac{m(v_i - v_f)}{(t_2 - t_1)} \quad \text{Eq. 6.3}$$

Here v_i and v_f is initial and final velocity of the projectile. The final velocity of the projectile, if there is no perforation, will be opposite direction of the initial due to *bounce back*. The time interval of steel on steel impact is quite low, which creates large impulse force.

Figure 9 all the different forces during an impact. Due to loss in kinetic energy from *damping force* and *friction force*, the angle of impact will be larger in relation to the horizontal than after the impact.

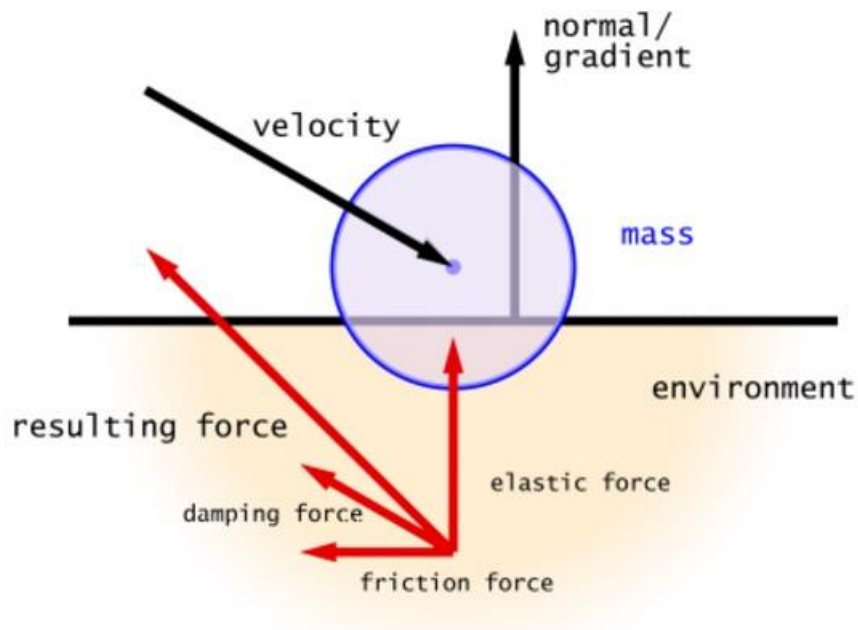


Figure 9 Decomposition of forces during impact

6.2 Bounce back

Elastic deformation in both projectile and target can create *bounce back*. During the collision, there is a deformation in the colliding elements, and bounce back is a result of restoration between the two. During the restoration, the elements will push each other apart. The energy in this rejection is mainly determined by the elasticity of the materials, initial kinetic energy and energy lost in plastic deformation as well as heat loss. A large bounce back is undesired as it might change the trajectory of the projectile and increase the severity of the situation. *Figure 10* shows how a projectile might act against a wall. The angle of the impact will change according to energy lost in the impact.

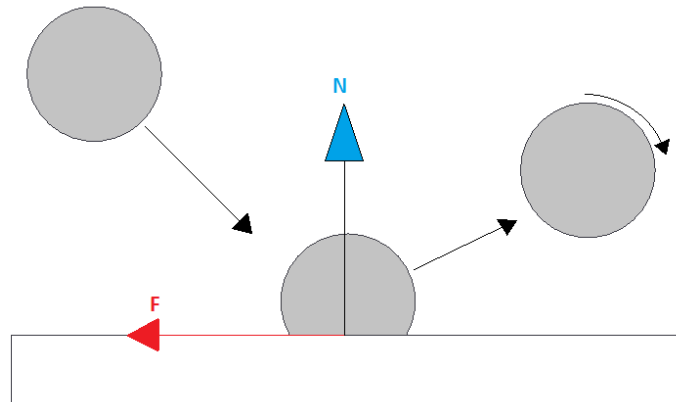


Figure 10 Ball bouncing

6.3 Coefficient of Residual energy

A way to determine an approximate value of residual kinetic energy is to use Coefficient of Residual energy (CoR). This value is based on the elastic value of the two colliding elements. The law of conservation of energy is used as a basis for the calculations. Energy is lost mainly due to heat energy and plastic deformation. CoR is given by *Eq. 6.4*.

$$CoR = \frac{v_f}{v_i} \quad Eq. 6.4$$

The law of conservation of energy (*Eq. 6.5*) dictates that no energy is lost.

$$E_{k1} = E_{k2} + H + W \quad Eq. 6.5$$

Here, E_{k1} is the kinetic energy of the projectile and E_{k2} is the residual energy after impact. H is thermal energy produced by the impact and W is the work performed on the target. The work creates deformation and can be calculated by *Eq. 6.6*.

$$W = \int_{L_1}^{L_2} F dx = F \cdot \Delta L \quad Eq. 6.6$$

Where F is the impulse force and ΔL . The energy from work can create both elastic and plastic deformation, depending on the quantity and material properties. The elastic deformation is the energy, which creates the bounce back.

The value of CoR for impact between two steel materials depends greatly on the velocity. The higher velocity the lower CoR. Results from Lifshitz & Kolsky (1964) and Thornton & Ning (1998) shows that for low velocities ($v < 10\text{m/s}$) the CoR is 90%. Impacts with higher velocity, 70 % or less of the projectiles energy is conserved as kinetic energy.

When confronted with angular impacts, it is necessary to decompose the forces into axial directions. Tangential impacts have much higher CoR, where usually 90 % of the energy remains kinetic energy. This value depends on the angle of the impact as well as velocity. One of the reasons for energy loss in tangential impacts is the friction force at the moment of impact. *Figure 11* shows the different phases in the impact. To the left, is before impact, the middle is during mostly elastic deformation and right is during mostly plastic deformation. The deformation as shown to the right indicates that there will be a lower coefficient of restitution.

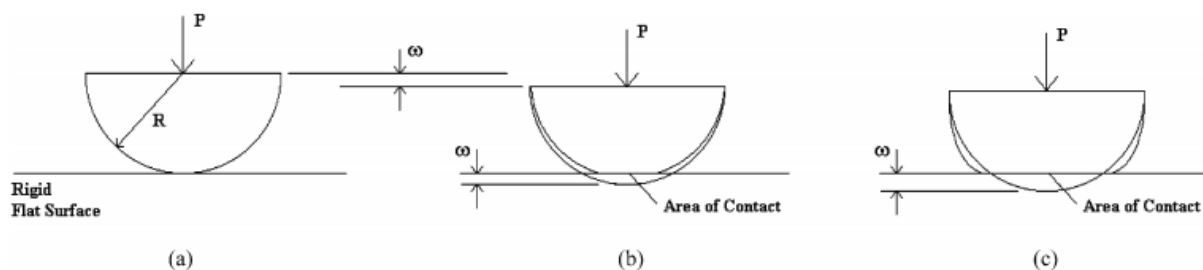


Figure 11 Spherical model during impact

6.4 Wall penetration by projectile

The calculations for predicting penetration is in most cases developed for concrete and rock. This is because concrete and rock is usually means of protection against missiles and bullets in war. The US army did extensive research on the subject during World War II. The largest issue with the subject is the giant spread in weight and velocity of the projectile as well as material strength and thickness of the target wall.

Most of the research is conducted with small, high velocity bullets in collaboration with the military, and is therefore outside scope of predicted hazards. Penetration, perforation and scabbing is based on the Teland, (1998) and Latif (2012).

The general formula for calculating penetration is given by the relationship between the diameter and penetration depth (Eq. 6.7).

$$\frac{x}{D} = \alpha \frac{M \cdot v^{\gamma_3}}{D^{\gamma_2} \cdot \sigma_c^{\gamma_1}} + \beta \quad \text{Eq. 6.7}$$

Where x is the penetration depth, D the diameter and M is the mass of the projectile. Further, v is the projectile's impact velocity and σ_c the compressive strength of the wall, while α , β and γ_i is various non-dimensional constants.

One of the issues is that since most of the results are empirical, the dimensions are uneven. As the left side is non-dimensional, the γ_i -constants on the right side have to be the following to meet the same requirement.

$$\gamma_1 = 1, \quad \gamma_2 = 3, \quad \gamma_3 = 2$$

This gives Eq. 6.8.

$$\frac{x}{D} = \alpha \frac{M \cdot v^2}{D^3 \cdot \sigma_c} + \beta \quad \text{Eq. 6.8}$$

The values of γ_i is a special case to satisfy the dimensions on both side. Table 6 shows the values in the most fundamental formulas for calculating penetration. The table is collected at Teland (1998)

Table 6 Fundamental penetration formulas

Formula	α	β	γ_1	γ_2	γ_3
Beth	$3.6 \cdot 10^{-4} N$	$0.5 N$	0.5	2.78	1.5
ACE	$3.5 \cdot 10^{-4} N$	0.5	0.5	2.785	1.5
NDRC modified	$3.8 \cdot 10^{-5} N$	1.0	0.5	2.9	1.8
Bernard (concrete)	$0.254 \cdot \rho^{-1/2}$	0	0.5	3.0	1.0

Here N is the “nosefactor” of the projectile. It describes the shape of the projectile, which is important to describe the penetration. The value of the “nosefactor” varies in the different calculations but stays in the range of $[0.7, 1.2]$. In Bernard's equation, ρ is the density of concrete.

There are some similarities in the formulas above, but they have all problem with uneven dimensions. Unfortunately, the data behind the Beth, ACE (Army Corps of Engineers) and NDRC (National Defense Research Committee) formulas was not released to the public, which have made it difficult to improve the formulas. Another issue is that these tests were performed at concrete with strength within the range of $[27, 44]$ MPa in World War II. That means that

the formulas might not describe the penetration correctly based on today's specifications. The velocity range is also outside the scope of what hazards that might occur.

The most important parameter considering penetration depth, is γ_2 , which describes the diameter of the projectile. The range between the values of the parameter is quite similar in the formulas. This is important for the validity of the results.

6.4.1 Adeli and Amin formula for penetration

Adeli and Amin (1985) developed a similar approach. The calculations mostly focused on flying objects against nuclear power plants. Further, they believed that to describe the penetration, it was necessary with either a quadric (Eq. 6.9) or a cubic polynomial (Eq. 6.10)

$$\frac{x}{D} = 0.0416 + 0.1698I - 0.0045I^2 \quad \text{Eq. 6.9}$$

$$\frac{x}{D} = 0.0123 + 0.196I - 0.008I^2 + 0.0001I^3 \quad \text{Eq. 6.10}$$

Where I , the impact factor, is defined by Eq. 6.11.

$$I = N \frac{Mv^2}{D^3 \sigma_c} \quad \text{Eq. 6.11}$$

The formula was made for the velocity range of $[27,311]$ m/s, mass range of $[0.1,343]$ kg and the range of impact factor is $[0.3,21]$. The diameter and the penetration ratio $\left(\frac{x}{D}\right)$ has to be less than 12 and 2 meter, respectively.

6.4.2 Hughes formula for penetration

Hughes (1984) also developed a formula. This formula (Eq. 6.12) was also dimensionally correct, but did not base the material strength on compression but rather the tension strength of the concrete.

$$\frac{x}{D} = \frac{0.19N}{1+12.3 \ln\left(1+0.03 \frac{Mv^2}{\sigma_t D^3}\right)} \cdot \frac{Mv^2}{\sigma_t D^3} \quad \text{Eq. 6.12}$$

Where σ_t is the tensile strength of concrete. The formula is applicable only if there is no *scabbing* or *perforation*. This formula also includes the impact formula, although it is not expressed by its symbol. For low impact values, the formula may predict too deep penetration.

6.4.3 Forrestal formula for penetration

Later a formula was created by Forrestal (1996), which is partly analytical. The projectile is assumed to act as a rigid body. Within the range $0 < x < 2D$, the force acting on the projectile is given by *Eq. 6.13*.

$$F = \pi \frac{D}{8} (\sigma_c \cdot S(\sigma_c) + N \cdot \rho_t \cdot V_1^2) x \quad \text{Eq. 6.13}$$

And for $x > 2D$ the force is expressed by *Eq. 6.14*.

$$F = \pi \frac{D^2}{4} (\sigma_c \cdot S(\sigma_c) + N \cdot \rho_t \cdot v^2) \quad \text{Eq. 6.14}$$

Where V_1^2 is given by *Eq. 6.15*.

$$V_1^2 = \frac{2M \cdot v^2 - \pi \cdot D^3 \cdot \sigma_c \cdot S(\sigma_c)}{2M + \pi \cdot D^3 \cdot N \cdot \rho_t} \quad \text{Eq. 6.15}$$

In these formulas, S is an empirical constant, which is a function of the compressive strength of concrete (*Eq. 6.16*).

$$S(\sigma_c) = 82.6 \left(\frac{\sigma_c}{10^6} \right)^{-0.544} \quad \text{Eq. 6.16}$$

S is, by definition, a non-dimensional constant, but this is not satisfied by the right-hand side of the equation. Further, the penetration depth is given by *Eq. 6.17*:

$$\frac{x}{D} = \frac{2M}{\pi \cdot D^3 \cdot \rho_t \cdot N} \ln \left(1 + \frac{N \cdot \rho_t \cdot V_1^2}{\sigma_c \cdot S(\sigma_c)} \right) \quad \text{Eq. 6.17}$$

The Forrestal formula have a good agreement to a lot of tests. The formula is the only one which fit for concrete with a stronger compressive strength than 50 MPa. Also the formula work best for smaller projectiles with high velocity.

6.4.4 Range of empirical formulas

Table 7 gives a collection of all the formulas for calculating the penetration. Most of these formulas are out of range, but they will give some guideline towards the penetration thickness. The range in this table applies for the formulas when calculating *perforation* as well as *scabbing*. The parameters that are missing should be chosen as reasonable values.

Table 7 Range of empirical formulas for calculating penetration of concrete

Formula	v [m/s]	M [kg]	D [m]	σ_c [MPa]	I	x/D
Beth	[200,1000]	-	[0.01-0.15]	[27,44]	-	-
Ace	[200,1000]	-	[0.01-0.15]	[27,44]	-	-
NDRC	[200,1000]	-	[0.01-0.15]	[27,44]	-	-
Bernard	[300,800]	[5.9,1066.0]	[0.08,0.26]	-	-	>3
Adeli & Amin	[27,311]	[0.1,343]	<12	-	[0.3,21]	<2
Hughes	<1050	-	-	-	<3500	-
Forrestal*	[277,945]	[0.1,0.9,5.9]	[0.01, 0.03, 0.08]	[11.7-15.0, 32.4-40.1, 90.5-108.3]	-	-

*The range is special since $M_{1.1}$ responds to $D_{1.1}$ and $\sigma_{c,1.1}$ in the matrix and so on.

6.4.5 Analytical model of penetration

In later years an analytical model of penetration has been developed by Li and Chen, Li (2003). The formula uses the same parameters as the previous formulas but include both compressive strength, tensile strength and density of the target concrete. The deceleration of the projectile is considered as linear due to neglecting the friction forces. The resistance force of the concrete in axial direction is in the initial phase ($\frac{x}{D} < k$) given by Eq. 6.18 and k is given by Eq. 6.19. This relation was developed by Forrestal (1994).

$$F_R = c \cdot x \quad \text{Eq. 6.18}$$

$$k = 0.707 + \frac{h}{D} \quad \text{Eq. 6.19}$$

Where k is a dimensionless parameter which describes the nose shape of the projectile, h is the nose length and c is according to Li (2003), a constant expressed by Eq. 6.20.

$$c = \frac{\pi \cdot D^2}{4k} \cdot \frac{S \cdot \sigma_c + N \cdot \rho \cdot v^2}{1 + N \cdot \rho \left(\frac{\pi \cdot k \cdot D^3}{4M} \right)} \quad \text{Eq. 6.20}$$

Where the unit of σ_c is MPa. Further, the resistance force for $\frac{x}{D} \geq k$ is given by Eq. 6.21.

$$F_R = \frac{\pi \cdot d^2}{4} (S \cdot \sigma_c + N \cdot \rho \cdot V^2) \quad \text{Eq. 6.21}$$

The final penetration depth for $\frac{x}{D} < k$ is, according to Li (2005) given by Eq. 6.22 and $\frac{x}{D} \geq k$ by Eq. 6.23.

$$x = v \sqrt{\frac{M}{c}} \quad \text{Eq. 6.22}$$

$$x = \frac{2M}{\pi \cdot D^2 \cdot N \cdot \rho} \ln \left(1 + \frac{N \cdot \rho \cdot v_1^2}{S \cdot \sigma_c} \right) + k \cdot d \quad \text{Eq. 6.23}$$

Where v_1 is given by Eq. 6.24.

$$v_1 = \sqrt{\frac{Mv^2 - \frac{\pi \cdot k \cdot D^3}{4} S \cdot \sigma_c}{M + \frac{\pi \cdot k \cdot D^3}{4} N \cdot \rho}} \quad \text{Eq. 6.24}$$

6.5 Wall perforation by projectile

The critical part in the case considered in this thesis is when the projectile perforates the wall. This is an undesirable situation, which could create a dangerous situation. *Figure 12* shows the damage after a high velocity small projectile perforated the wall. Unfortunately, it was not possible to obtain any information regarding the projectile or its velocity. Further, the figure show how the reinforcement was deformed and cut by the projectile. The test was performed with water pressure at 3000 bar, but the size of the pressurized vessel was not stated. The pictures were given with the permission from the owner.



Figure 12 Penetration of safety walls

To predict the necessary wall thickness to prevent perforation it is necessary to look at the relation with penetration. What will be important is to decide a sufficient wall thickness and in worst case calculate the residual energy of the projectile.

6.5.1 NDRC formula for perforation thickness

The National Defense Research Committee (NDRC) developed a formula by Chelapati and Kennedy (1972), to describe the perforation thickness (*Eq. 6.25* and *Eq. 6.26*).

$$\frac{h}{D} = 1.24 \frac{x}{D} + 1.32, \quad 1.35 < \frac{x}{D} < 13.5 \quad \text{Eq. 6.25}$$

$$\frac{h}{D} = 3.19 \left(\frac{x}{D}\right) - 0.718 \left(\frac{x}{D}\right)^2, \quad \frac{x}{D} < 1.35 \quad \text{Eq. 6.26}$$

Here $\frac{x}{D}$ is the penetration depth calculated in the *NDRC formula for penetration*. Chang (1981) argues that the perforation formula by NDRC is too conservative.

6.5.2 Chang formula for perforation

Chang's formula (*Eq. 6.27*) was derived in 1981 mostly classical mechanic methods. To determine some constants, he based them on test data.

$$h = 2.79 \sqrt{\frac{M}{D^3 \sigma_c}} v^{0.75} \quad \text{Eq. 6.27}$$

Where h is the notation for perforation thickness. The range this formula is applicable for is projectile velocity v between [16.7,311.8] *m/s*, projectile mass M between [0.1,343.6] *kg*, concrete compressive strength σ_c between [23.2,46.4] *MPa* and projectile diameter D between [20,305] *mm*.

6.5.3 Hughes formula for perforation

Hughes (1984) developed *Eq. 6.28* and *Eq. 6.29* to describe the perforation of concrete.

$$\frac{h}{D} = 3.6 \frac{x}{D}, \quad \frac{x}{D} < 0.7 \quad \text{Eq. 6.28}$$

$$\frac{h}{D} = 1.58 \frac{x}{D} + 1.4, \quad \frac{x}{D} > 0.7 \quad \text{Eq. 6.29}$$

The validity rang of his perforation formula is the same as the penetration formula. The value of $\frac{x}{D}$ is predicted by Hughes penetration formula as well.

6.5.4 Adeli and Amin formula for perforation

Adeli and Amin (1985) determined that perforation could be explained with a cubic equation (*Eq. 6.30*) similar to how they explained penetration.

$$\frac{h}{D} = 0.906 + 0.3214I - 0.0106I^2 \quad \text{Eq. 6.30}$$

Both the impact factor and the range of validity is the same as their formula for penetration.

6.6 Wall scabbing

Scabbing is defined as the end section of the wall getting pushed out by the projectile. The section, which is discharged, is often larger than the diameter of the projectile.

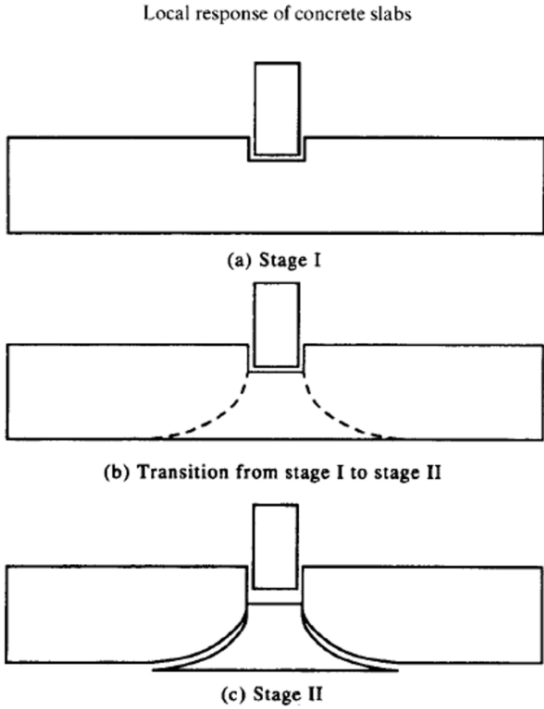


Figure 13 A two-stage perforation model

Figure 13 illustrate a projectile penetrating a concrete wall, where the end section is separated from the wall. This is referred to as scabbing. The thickness of the released section is the scabbing thickness s .

6.6.1 NDRC formula for scabbing

Eq. 6.31 and *Eq. 6.32* was derived by Chelapati and Kennedy (1972), and was developed years after the tests were conducted.

$$\frac{s}{D} = 7.91 \frac{x}{D} - 5.06 \left(\frac{x}{D}\right)^2, \frac{x}{D} < 0.65 \quad \text{Eq. 6.31}$$

$$\frac{s}{D} = 2.12 + 1.36 \frac{x}{D}, 3 < \frac{s}{D} < 18 \quad \text{Eq. 6.32}$$

6.6.2 Chang formula for scabbing

To calculate the scabbing thickness Chang (1981) devised *Eq. 6.33*.

$$s = 3.14 \left(\frac{M}{D^3 \sigma_c}\right)^{0.4} v^{0.67} \quad \text{Eq. 6.33}$$

6.6.3 Hughes formula for scabbing

Hughes (1984) derived *Eq. 6.34* and *Eq. 6.35* for scabbing thickness based on his calculations on penetration and perforation.

$$\frac{s}{D} = 5.0 \frac{x}{D}, \frac{x}{D} < 0.7 \quad \text{Eq. 6.34}$$

$$\frac{s}{D} = 1.74 \frac{x}{D} + 2.3, \frac{x}{D} > 0.7 \quad \text{Eq. 6.35}$$

6.6.4 Adeli and Amin formula for scabbing

Eq. 6.36 is the Adeli and Amin (1985) formula for scabbing. The formula is based on curve fitting from results.

$$\frac{s}{D} = 1.8685 + 0.4035I - 0.0114I^2 \quad \text{Eq. 6.36}$$

Where I is the same as in the penetration and perforation formulas.

6.7 *Review of the formulas*

According to *A review of empirical equations for missile impacts on concrete* [ref] from the Norwegian defence institute, the most accurate of the empirical formulas would be the ones developed by Adeli & Amin. Unfortunately, the formulas are based on low impact velocities, and may then not be accurate for many of the smaller projectiles possible. Even for low velocity impacts, the calculations should have some reservations due to many uncertainties in the results.

For smaller projectiles, which have higher velocity, there is a greater need for accurate results. Almost all high velocity impact data are from the American tests during World War II. This means that the calculations will have a large uncertainty, as both concrete and ballistic technology has come a long way.

In this thesis, the penetration will be predicted by the analytical model from Li and Chen. The model does not take consideration of perforation or scabbing. To back up Li and Chen's formula if any of the results is unrealistic the empirical formulas will act as a comparison.

The calculation regarding perforation of the safety walls is important when estimating the safety level. Unfortunately, the behavior of the structure is quite hard to predict. The penetration of the wall is therefore based mostly if the penetration depth exceeds the wall thickness

The calculation of scabbing is quite uncertain and the result from these calculations will not be emphasized during the results. This mainly because of old formulas with outdated properties.

7 Test of projectile discharge

This chapter presents the experiment conducted as part of this thesis work. The objective of this experiment is to determine the amount of energy in a pressurized vessel, which is transferred into kinetic energy during failure. This is to get a better understanding of an actual failure. Another reason for conducting the test was to illustrate how much energy a test contains. The test will be conducted with different pressures to compare more data.

To measure the energy, a projectile with a weakened fastening is put at the end of a pipe. The assembly (*Figure 14*) is designed so the strength of the fastening is adjustable.

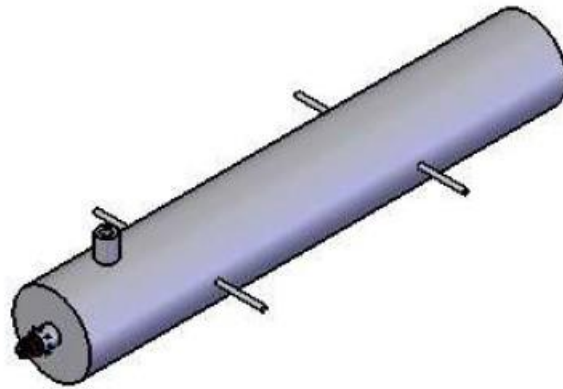


Figure 14 Model of test-assembly

The aim with this experiment is to examine the relationship between theory and practice of pressure testing. There are different theories to the energy release in a failure of a vessel, and hopefully during this test a comparison is possible. The largest issue is how much of the potential energy in the pressurized vessel is transformed into kinetic energy.

7.1 Testing procedure

The test was performed with hydrostatic pressure inside a pipe. One of the end sections had a projectile, which was fastened with M3-pins. This is shown in *Figure 15*. The left side show the projectile section in the drawing, while the right photo is from the actual test. The number of M3-pins was adjustable to conduct the test under different conditions. When the pins failed, the projectile was released from the pressure vessel. The aim was to calculate the kinetic energy in the projectile by measuring the trajectory after failure.

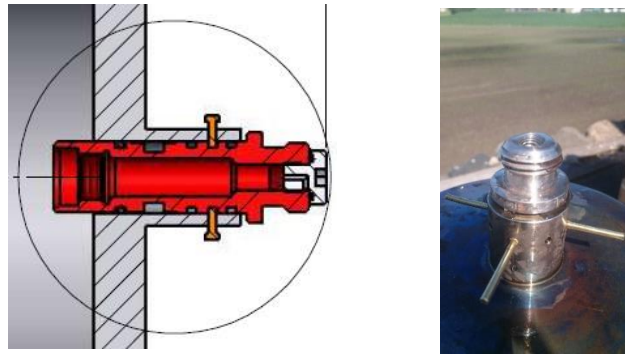


Figure 15 Projectile with pins:

To contain the different hazards identified in a pressurized vessel a job safety analysis was performed. The procedure and job safety analysis made in collaboration with T.D. Williamson is in *Appendix C*. The pressurized pipe was placed inside a larger steel pipe to prevent hazards directed towards the operational area. The projectile was facing an open area and the other end was facing a steel container. All personnel and essential equipment was placed behind a concrete safety wall. The test vessel was connected to a data log, which read the inside pressure. *Figure 16* shows the test area and the test assembly.



Figure 16 Test-assembly with protective pipe

The test was conducted several times with different number of fasteners. Due to a time limit, the test was only conducted for three different scenarios through five tests in total. Firstly, the test-rig was prepared according to the assembly in *Appendix C* and placed according to the model of the test area. In each test, the vessel was filled with water and before the projectile was fixed, it was ensured that there was no air trapped inside. The projectile was fixed with 3 mm pin(s) of brass. When the test rig was prepared for launch, it was put inside a pipe to give a protective barrier in case of rupture and was placed in horizontal position. The recording device were activated and when all personnel were behind the safety wall, the vessel was put under pressure. The pressure was gradually increased until burst of projectile. Due to more energy in the tests than expected, the maximum amount of pins was three.

7.2 *Equipment*

For this test, the following equipment are used:

- Projectile (2)
- Watertight vessel
- Data log
- Compressor/pressure transmitter
- O-rings (20)
- M3-pins in brass (50-60)
- Water supply
- Electricity
- Level
- Personal Protective Equipment (Glasses, helmet, hearing protection, protective footwear, gloves)
- Distance measurement device
- Camera equipment (Gopro, tripod)
- Visualized aid for camera: Steel wire and papers

Drawings of projectile and pressure vessel as well as datasheet for the Brass M3-pins is collected in Appendix C.

7.3 Preliminary calculations

To get an estimate of the different expected energy levels during the test a set of preliminary calculations were performed. The calculations involve ultimate shear strength (USS) on the M3-pins, force to pressure relation, expected projectile trajectory and potential energy in the test.

7.3.1 Ultimate shear strength Brass M3-pins

Table 8 gives an overview over the results in this section. The results are calculated by the formulas in this chapter.

Table 8 Results preliminary calculations M3-Pins

	Symbol	Value
Ultimate tensile strength [MPa]	σ_{UTS}	338 – 469
Ultimate shear strength [MPa]	τ	230 – 319
Diameter pin [m]	D_{bolt}	0.003
Diameter projectile [m]	D_{proj}	0.027
Force/bolt [N]	F_{bolt}	1626 – 2255
Pressure [bar/bolt]	P_{bolt}	28.4 – 39.4
Max pressure 8 pins [bar]	P_{max}	227.2-315.1

Table 9 give the relation between UTS and USS. The table also give the relation between shear yield strength (SYS) and tensile yield strength (TYS)

Table 9 Ultimate tensile strength vs Ultimate shear strength

Material	Approx. relationship between USS and UTS	Approx. relationship between SYS and TYS
Steels	USS = 0.75 · UTS	SYS = 0.58 · TYS
Ductile Iron	USS = 0.9 · UTS	SYS = 0.75 · TYS
Malleable Iron	USS = 1.0 · UTS	
Wrought Iron	USS = 0.83 · UTS	
Cast Iron	USS = 1.3 · UTS	
Aluminum	USS = 0.65 · UTS	SYS = 0.55 · TYS
Brass	USS = 0.68 · UTS	

Ultimate shear strength from ultimate tensile strength (Eq. 7.1).

$$\tau = 0.68 \cdot \sigma_{UTS} \quad \text{Eq. 7.1}$$

Ultimate Shear strength is expressed by Eq. 7.2.

$$\tau = \frac{F}{A_{pin}} = \frac{4 \cdot F}{\pi \cdot D_{pin}^2} \quad Eq. 7.2$$

From this relation it is possible to find the pressure acting on the projectile (Eq. 7.3).

$$F_{pin} = P_{pin} \cdot A_{proj} = \frac{\tau \cdot \pi \cdot D_{pin}^2}{4} \quad Eq. 7.3$$

The pressure necessary for failure by each pin is expressed by Eq. 7.4.

$$P_{pin} = \frac{\tau \cdot \pi \cdot D_{pin}^2}{4 \cdot A_{proj}} = \frac{\tau \cdot D_{pin}^2}{D_{proj}^2} \quad Eq. 7.4$$

The maximum theoretical pressure (Eq. 7.5) during the test.

$$P_{max} = P_{pin} \cdot 8 \quad Eq. 7.5$$

The pins are brass, with an UTS between 338 and 469 [MPa]. Error-sources in these calculations include the actual UTS, the relation between UTS and USS as well as friction forces in the fitting of the projectile.

7.3.2 Calculation of potential energy in the vessel

Different theories from *Ch. 5* under projectile discharge are considered in these calculations. The properties and results of the test are given in *Table 10* and *Table 11*, respectively.

Table 10 Results of preliminary calculations Baker equation

	Symbol	Value
Volume vessel [m ³]	V	0.0187
Pipe radius to wall thickness ratio	δ	5.426
Water density [kg/m ³]	ρ	1000
Bulk modulus water [Pa]	β	$2.2 \cdot 10^9$
Compressibility water [1/Pa]	C	$4.55 \cdot 10^{-10}$
Number of bolts	n	8
Energy Baker Equation [J/pin]	E_B	$(34.3 - 66.0) \cdot n^2$

Table 11 Preliminary calculation results based on first law of thermodynamics

Pressure [bar]	Specific Volume [m ³ /kg]	Energy PdV
0	0.001002	0
40	0.001000	131.8
80	0.000988	581.9
120	0.000988	1320.5
160	0.000996	2238.1
200	0.000993	3394.4
220	0.000992	4062.1

The elastic energy in the pipe was not included as it was small compared to the potential energy of the compressed water. The results show that the *Baker equation* give a significantly lower potential energy for each pin.

7.3.3 Calculation of trajectory

The results from the equations in this section is gathered in *Table 12*. The results are based on calculations from the *Baker equation* and the *first law of thermodynamics* as well as Manning (2005) on the relation between potential energy and kinetic energy of a projectile. This relation says that the kinetic energy in a projectile will have 20% of the total energy from the calculations using the *Baker formula*.

Table 12 Preliminary trajectory results

	Symbol	Value	Trajectory length ($z = 1$)**
Mass [kg]	m_{proj}	0.35	-
Initial velocity 1 pin Baker [m/s]	v_{B_1}	6.3 – 8.8	2.8 – 4.0
Initial velocity 2 pins Baker [m/s]	v_{B_2}	12.5 – 17.6	5.6 – 7.9
Initial velocity 3 pins Baker [m/s]	v_{B_3}	18.8 – 26.4	8.5 – 11.9
Initial velocity 4 pins Baker [m/s]	v_{B_4}	25.0 – 35.2	11.3 – 15.9
Initial velocity 5 pins Baker [m/s]	v_{B_5}	31.3 – 44.0	14.1 – 19.9
Initial velocity 6 pins Baker [m/s]	v_{B_6}	$37.6 - n/a^*$	$17.0 - n/a^*$
Initial velocity 7 pins Baker [m/s]	v_{B_7}	$43.8 - n/a^*$	$19.8 - n/a^*$
Initial velocity max pressure [m/s]	$v_{B_{max}}$	48.4	21.9
Initial velocity 1 pin Therm. [m/s]	v_{T_1}	12.3	5.6
Initial velocity 2 pins Therm. [m/s]	v_{T_2}	25.8	11.6
Initial velocity 3 pins Therm. [m/s]	v_{T_3}	38.8	17.5
Initial velocity 4 pins Therm. [m/s]	v_{T_4}	50.6	22.8
Initial velocity 5 pins Therm. [m/s]	v_{T_5}	62.3	28.1
Initial velocity max pressure [m/s]	$v_{T_{max}}$	68.1	30.7

*Calculations of Thermodynamic formula is based on highest pressure, *maximum allowable pressure is 220 bar, **All dimensions are in [m]*

Usually the *Baker formula* has been used as basis when calculating energy, and the projectile distance was not expected to exceed 30 meters. To calculate the potential energy into kinetic energy *Eq. 5.28* was used. From this we could calculate the velocity of the projectile.

To calculate the length of the trajectory it is necessary to use the same method as in *Chapter 5* regarding *a water jet*. Since the vessel is assumed to be completely leveled, the height is given by *Eq. 7.6*.

$$z = \frac{1}{2} a \cdot t^2 \quad \text{Eq. 7.6}$$

When calculating the trajectory of the projectile the air resistance is neglected.

7.4 Test results

The results of the projectile had larger kinetic energy than expected. Therefore, due to safety considerations, the maximum amount of pins used during the test was three. Due to quite uneven terrain, the height of impact zone was quite hard to measure. Therefore, the velocity of the projectile was measured with a camera and a scale. The camera took 120 photos per second, and the stick was 2.5 meters. With this equipment it was possible to calculate the velocity of the projectile. *Figure 17* shows the captions of the test were the projectile had the highest velocity. The figure shows how a water jet will dissipate during a discharge.



Figure 17 Captions of projectile discharge during test

Table 13 Test results

Test	Pin	Pressure [bar]	Length [m]	Velocity [m/s]	Note
1	1	2	5	9	Projectile insufficient fastened
2	1	43	12	25	Height approx. 1 meter
3	2	75	44	44	Height approx. 2.6 meter
4	2	80	43	46	Height approx. 2.6 meter
5	3	133	65	63	Height approx. 2 meter

Table 13 gives the results from the test. The first test conducted the pin were not properly fastened to the projectile, which led to an early discharge under low pressure. That test is therefore excluded from the results as a deviation.

7.5 Discussion of results

Due to larger kinetic energy than expected, the results show that more than 20% of potential energy is transformed into kinetic energy. Also, the pins withstood larger forces than the calculations predicted.

Table 14 Comparison of test results and calculations

	Pressure [bar]	Test [m/s]	Baker [m/s]	Therm. [m/s]	Note
1	2	9	-	-	Excluded
2	43	25	21	29	Baker (-4), Therm. (+4)
3	75	44	37	54	Baker (-7), Therm. (+10)
4	80	46	39	58	Baker (-7), Therm. (+12)
5	133	63	65	95	Baker (+2), Therm. (+33)

Table 14 gathers the results from the test together with the calculations from the *Baker formula* and the *first law of thermodynamics*. It is assumed in these calculations that all of the potential energy inside the test is transformed into kinetic energy in the projectile.

The results show that *Baker formula* gives the most accurate representation of the results. It shows a lower velocity for all except the last test, but this may be since the material elastic energy has not been included. The pump may also have a larger effect on the projectiles at lower pressure rates. The *first law of thermodynamics* gives quite the conservative velocities, and this is without the energy from change of *entropy*? Inside the vessel and the elastic material energy.

Figure 18 shows the calculations and test results in a graph. This shows how similar the energy in the *Baker formula* and the *first law of thermodynamics* increase quite similarly. When looking at the results of the tests, the increasing kinetic energy in the projectile follows the same trend as the calculations until the last test. Here, the velocity is lower than what the calculations indicate. This may be due to different error-sources.

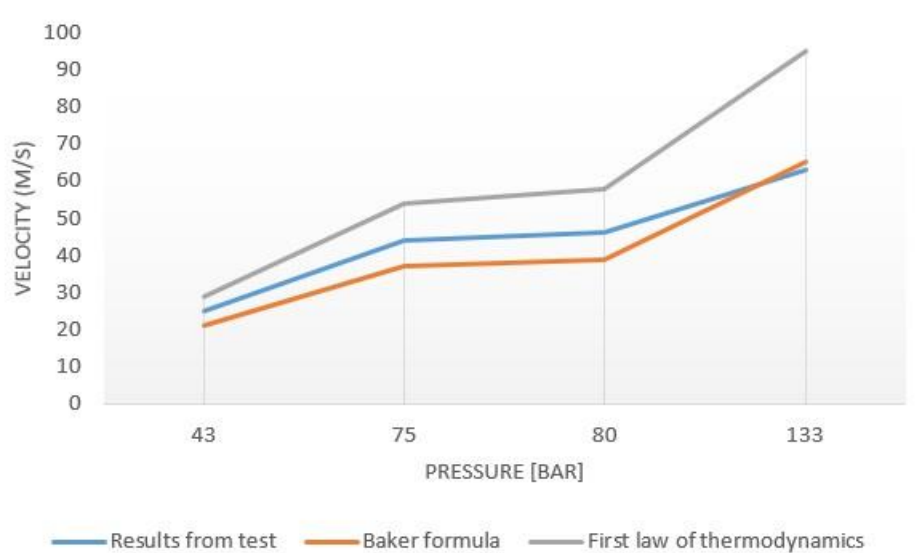


Figure 18 Graph of projectile velocity from test and calculations

Due to many uncertain elements during the test, we have a lot of error-sources. Therefore, the results will only be used as a guideline to which method to use later in the thesis. Here are the error-sources that might have had some impact on the results:

1. During the discharge, the pressure vessel is pushed back from the energy released. Therefore, some of the energy in the discharge is transferred over to the vessel.
2. The pump used in the testing is quite coarse so fine tuning when reaching max pressure was difficult. Therefore, the continuous flow from the pump adds to the change in volume and give the projectile more kinetic energy. This will most likely happen during a normal pressure test, so the energy should be included, but the formulas do not take this into account.
3. The vessel might not have been completely horizontal during discharge, and therefore the length might be longer or shorter and give inaccurate results.
4. Uncertainty in the results as the test was only conducted one or two times for each situation.
5. Air resistance and wind changes the velocity of the projectile. The air resistance force and wind force is uncertain elements acting on the projectile during its trajectory. It is hard to determine both as the wind speed is not known, as well as the shape coefficient on the projectile changes since the projectile starts to rotate during the trajectory.
6. Uncertainty in pressure measuring equipment. The data-log might show inaccurate pressure.

Smaller error sources include:

1. Friction acting on the projectile during discharge. The projectile is fitted to the vessel so there is no leak. This will create friction during discharge and will give some reduction in kinetic energy in the projectile.
2. Inaccurate measurement of distance and height. Due to quite large trajectory, and variable terrain, the measurement of the distance was difficult. This method of calculating the velocity was not used because of uncertainty in distance and height. It is therefore considered as a minor error source.

From the results the *Baker formula* seems to be the best fit. If the elastic energy of the material is included as well, the formula will give a more conservative indication of the energy inside a pressurized vessel. This was not included in the results because of the number of error-sources.

8 Total energy during pressure testing

Based on the results from the test, the thesis will use the *Baker formula* when calculating the potential energy inside a pressurized vessel. The pressure tests used as a basis for calculating the strength of the walls is a *500 bar structural test on a Smartlay* and a *200 bar Factory Acceptance Test (FAT) of a 48" Smartplug*. These have the largest potential energy of the pressure tests conducted at T.D. Williamson Offshore Services. **Appendix Testing pipes** shows drawings and specifications of the pipes.

8.1 200 bar FAT-test Smartplug

The *200 bar FAT-test of a 48" Smartplug* is the test with the largest potential energy. This is because of large volume. *Table 15* gives the specifications of the pipe and test:

Table 15 The 200 bar FAT-test of a 48" Smartplug

Pipe: API X70	Symbol	Value
Inner Diameter [m]	ID_{FAT}	1.153
Thickness pipe [m]	T_{FAT}	0.041
Diameter ratio	δ_{FAT}	14.06
Length [m]	L_{FAT}	6.00
Test pressure [bar]	P_{FAT}	200
Cross-sectional area [m ²]	A_{FAT}	1.044
Volume [m ³]	V_{FAT}	6.265
Yield stress of pipe [MPa]	$\sigma_{y,FAT}$	485
Young's modulus [GPa]	E_{FAT}	206
Poisson ratio	ν_{FAT}	0.3
Mass plug [kg]	$m_{plug,FAT}$	6000
Mass end section [kg]	$m_{end,FAT}$	900*
Baker [J]	$E_{B,FAT}$	569517
Thermodynamics [J]	$E_{T,FAT}$	1140174
Elastic energy Material [J]	$E_{M,FAT}$	162616
Energy used in thesis [J]	E_{FAT}	732133

* Approximate value

From the results in the test, the elastic energy of the material and *Baker formula* give a good representation of the energy inside a test.

8.2 500 bar structural test Smartlay

The test with the highest pressure is a *500 bar structural test on a Smartlay*. The pressure is larger than the previous test but the pipe has a smaller cross-section and length. The properties of the test is given in *Table 16*.

Table 16 Properties of 500 bar structural test Smartlay

Pipe: API X65	Symbol	Value
Inner Diameter [m]	ID_{str}	0.741
Thickness pipe [m]	T_{str}	0.105
Diameter ratio	δ_{str}	9.06
Length [m]	L_{str}	1.00
Test pressure [bar]	P_{str}	500
Cross-sectional area [m ²]	A_{str}	0.4312
Volume [m ³]	V_{str}	0.4312
Yield stress of pipe [MPa]	$\sigma_{y,str}$	485
Young's modulus [GPa]	E_{str}	206
Poisson ratio	ν_{str}	0.3
Mass plug [kg]	$m_{plug,str}$	1300
Mass end section [kg]	$m_{end,str}$	400*
Baker [J]	$E_{B,str}$	245027
Thermodynamics [J]	$E_{T,str}$	476528
Elastic energy Material [J]	$E_{M,str}$	199131
Energy used in thesis [J]	E_{str}	444158

* Approximate value

Even with more than twice the pressure, the test in Ch. 7 contains more potential energy. This shows the significance of volume as well as pressure in terms of energy in a pressure test. The elastic energy of the pipe is also less than the previous test. This is because the area on which the pressure acts is smaller in the *structural test* than in the *FAT test*.

8.3 Pressure wave result

The pressure wave created from a rupture of the pipe can be calculated into weight of TNT. Through *Eq. 5.13* and *Eq. 5.14* the weight of TNT and the safety zone can be calculated for the tests considered in this thesis. The results are given in *table 17*.

Table 17 Result of pressure wave

Test:	Weight TNT [g]	Risk of eardrum rupture [m]	Safe distance [m]
200 bar FAT-test Smartplug	150.955	2.40	31.95
500 bar structural test Smartlay	91.579	2.03	27.04

The results in *Table 17* is only valid if all the potential energy inside a pressure vessel is transformed into a pressure wave. To create a pressure wave of this magnitude, all the energy has to be released at the same time. Therefore, the wave with significant magnitude will only occur during a total collapse of pipe or discharge of an end section. *Table* (From lees') shows how much of the energy is transferred into kinetic energy and pressure wave in such a failure. The calculations do not consider obstacles, such as safety walls, which result in a higher theoretical safe distance.

8.4 Water jet result

A hazard involving a water jet can be calculated through the formulas in *Chapter 5.2*. The velocity of the water jet is calculated through the transformed Bernoulli's formula expressed in *Eq. 5.16*. A simplification of *Eq. 5.16* for discharge through a small orifice is given by *Eq. 5.20*.

The trajectory of the jet is calculated through *Eq.*, *Eq.* and *Eq.*, which gives the maximum distance travelled, distance for any give angle and distance for a horizontal jet, respectively.

The results from the velocity and trajectory is given in *Table 18*. These results do not include air resistance or the disintegration in the jet. The usual assumption is that the actual travel distance of the jet is halved to dimidiation by drag force and disintegration Manning (2005).

Table 18 Water jet results

Test (height: $z = 1$ [m])	Velocity [m/s]	Trajectory horizontal discharge [m]	Max distance [m]
200 bar FAT-test Smartplug	120	54.2*	733.9*
500 bar structural test Smartlay	190	85.7*	1834.9*

*The distance is unrealistic as the jet will dissipate at such velocities. The drag force will also influence the jet greatly.

The distance of the travelled jet is quite large. The water jet will not be able to do any significant damage to the wall. This is due to the change in volume is small and the velocity of the jet will decrease quickly because of diminishing pressure after failure. An angle at discharge that gives a jet the trajectory that elude the wall, will have lost most of its kinetic energy before it reaches ground level. Therefore, the water jet will not be considered a hazard with the same risk level as a projectile.

9 Design of Safety walls

When developing a design, it is important to consider the limiting factors and the area of application. Sections of the walls should be portable, which require reasonable weight and a practicable way of movement. The transporting options are a 15-ton bridge crane and a forklift with maximum capacity at 8-10 ton. To make testing more efficient it is also important that the safety walls are easy to install and remove.

Another limiting factor is the cost. The development of the design should be based on ALARP, which in terms of cost, means that the outcome of the measure should reflect the cost. The main cost depending areas is choice of material, production cost and functionality features.

9.1 *Choice of materials*

When choosing the material for the walls there are important factors to consider. The material strength and ductility in both elastic and plastic deformation is important. Energy is absorbed through deformation, heat loss and friction force. A material that allow large deformation is therefore desirable for this purpose. Elastic deformation will make a projectile bounce back when it is restored to its original shape. With plastic deformation, the energy goes into permanently changing the structure. A material which have large plastic elongation is desired as it will absorb more energy.

9.1.1 Steel barrier

One choice of material is steel. The advantage with steel, is low density compared to strength and the ability to withstand shear and tension forces. Disadvantages are cost, both in material but also in production. Steel also have a large coefficient of restitution as well as great impulse force because of small time interval during the impact. Steel is a material with high elasticity and with the right alloy it can provide a good barrier. Preferable, a steel alloy with high toughness.

Austenitic steels are quite suitable since many have high tensile strength and allows for large plastic deformation. Two quite suitable austenitic steels are 304 and 316. AISI 304 have a tensile strength of 505 MPa and an elongation of 70% at break. AISI 316 has on the other hand a tensile strength of 580 MPa, but an elongation of 50%. The ductility of these materials make them suitable to absorb energy from impacts. The downside of these steels is that they are quite expensive.

A cheaper material which also may be an option is the s355. It is a steel which handle impact loads quite well. The tensile strength varies from 490 to 630 MPa depending on the material. This steel has only an elongation of 18%, which makes the austenitic steels more suitable.

In a collision between two elements the elastic energy could be considered as a spring force (Eq. 9.1).

$$F = k \cdot x \quad \text{Eq. 9.1}$$

Where F is the spring force, k is the spring coefficient and x is the deformation. If the cross-sectional area of the “spring” is included, Eq. 9.2 is transformed into Hooke’s law.

$$\sigma = E \cdot \varepsilon \quad \text{Eq. 9.2}$$

From Hooke’s law for spring force the work done to compress a spring is given by Eq. 9.3.

$$A = \int k \cdot x \, dx = \frac{1}{2} k \cdot x^2 \quad \text{Eq. 9.3}$$

To calculate the energy in the impact it is necessary to calculate the work applied on the two colliding elements (Eq. 9.4).

$$U_{el} = \frac{1}{2} E \cdot \varepsilon^2 = \frac{\sigma^2}{2E} \quad \text{Eq. 9.4}$$

Where U_{el} is the energy absorbed by elastic deformation in the steel. The absorbed is expressed as work per unit of volume of the deformed material. To calculate the volume of the deformation as shown in Figure 19, it is necessary to use the elongation of the material. Elongation is connected to the thickness of the wall (Eq. 9.5)

$$h_w = t_w \cdot e \quad \text{Eq. 9.5}$$

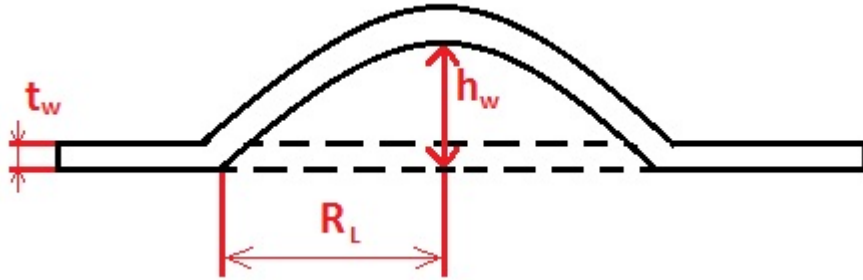


Figure 19 Local deformation in wall

Here h_w is the radius of the deformation as shown in Figure, t_w the wall thickness and e the elongation of the steel. The deformation shape is assumed to be similar to a paraboloid where the volume is given by Eq. 9.6.

$$V_w = \frac{\pi \cdot R_L^2 \cdot h_w}{2} \quad \text{Eq. 9.6}$$

Where V_w is volume of the paraboloid and R_L is the radius of the local deformation zone.

Another way to calculate the ability to resist impact or toughness of the material, is to look at the energy absorbed in stressing to fracture. The energy absorbed is equal to the area

under the stress-strain curve as shown in *Figure 20*. The figure shows the difference in area of a ductile and a brittle material.

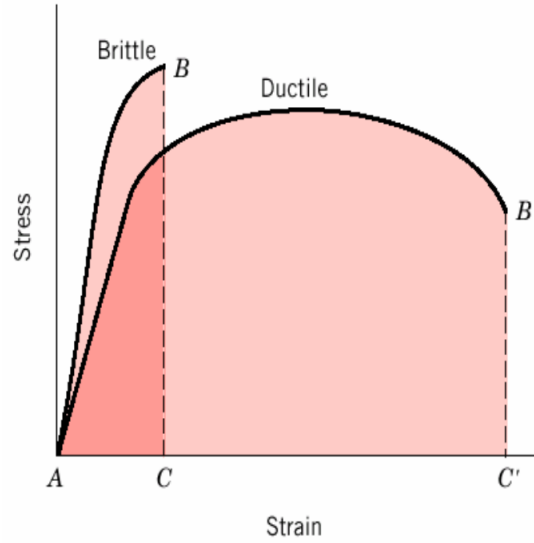


Figure 20 Area under stress-strain curve

The modulus of toughness based on engineering stress is given by the area in *Eq. 9.7*.

$$T_{Eng} = \int_0^{\varepsilon_f} \sigma d\varepsilon = \frac{1}{2} \int_0^{\varepsilon_y} \sigma_y d\varepsilon + \int_{\varepsilon_y}^{\varepsilon_f} \sigma_y d\varepsilon + \frac{\pi}{2} \int_{\varepsilon_y}^{\varepsilon_f} (\sigma_{UTS} - \sigma_y) d\varepsilon \quad Eq. 9.7$$

Where T_{Eng} is the engineering toughness of the material, ε_f is the strain at fracture of the wall, σ_y and ε_y is the yield strength and strain at yield of the material, respectively. Strain before fracture is calculated by *Eq. 9.8*.

$$\varepsilon_f \cdot A_w = A_e - A_w \quad Eq. 9.8$$

Which transforms to *Eq. 9.9*.

$$\varepsilon_f = \frac{\sqrt{R_L^2 + h_w^2} - R_L}{R_L} \quad Eq. 9.9$$

Here A_e is the surface area of the paraboloid and is given by *Eq. 9.10*.

$$A_e = 2\pi\sqrt{R_L^2 + h_w^2} \quad Eq. 9.10$$

Further, the energy is calculated through *Eq. 9.11*.

$$E_s = T \cdot V_w \quad Eq. 9.11$$

Where E_s is energy from deformation of the steel walls and V_s is the volume of the deformation.

Using the engineering stress is a conservative way to calculate the toughness during impulse load. Energy absorbed during impact is determined by true stress and true strain.

According to [ref], the relationship between engineering stress and strain compared to true stress and strain, is expressed by Eq. 9.12 and Eq. 9.13:

$$\sigma_{True} = \sigma_{UTS}(1 + \varepsilon_f) \quad Eq. 9.12$$

$$\varepsilon_{True} = \ln(1 + \varepsilon_f) \quad Eq. 9.13$$

Where σ_{True} is the true stress and ε_{True} is the true strain. Further the area under the curve is calculated by Eq. 9.14.

$$T_{True} = \frac{1}{2} \int_0^{\varepsilon_y} \sigma_y d\varepsilon + \frac{1}{2} \int_{\varepsilon_y}^{\varepsilon_f} \sigma_y + \sigma_{True} d\varepsilon \quad Eq. 9.14$$

Here T_{True} is the toughness during impact. The change in true stress-strain rate is considered to be linear after yield. The absorbed energy is given in Table 19.

Table 19 Steel properties

	Yield strength [MPa]	Eng. strain	True strain [m/m]	True stress [MPa]	T_{True} [J/m ³]
S355	355	0.15	0.14	627	$6.247 \cdot 10^7$
AISI 316	290	1.41	0.88	1400	$7.296 \cdot 10^8$
AISI 304	215	1.53	0.93	1275	$6.801 \cdot 10^8$

The energy is then given by Eq. 9.15, where U_s is the absorbed energy by the steel wall.

$$U_s = T_{True} \cdot V_w \quad Eq. 9.15$$

The radius of the local deformation is estimated based on the projectile diameter. For simplification purposes, the diameter of deformation is considered to be twice the projectile diameter. Figure 19 shows the perforation of a 4 mm thick steel plate with small projectiles. The initial velocity of the projectiles was 200, 316 and 580 [m/s], respectively.

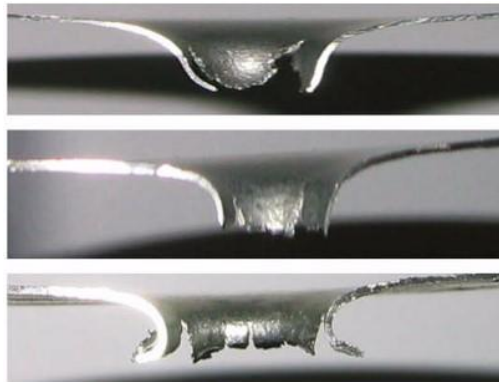


Figure 21 Perforation thin steel plate

The shear and moment capacity of the wall will only be an issue when considering a larger projectile. A small projectile will only influence the wall on a local scale, due to moment of inertia in the wall. A large projectile is defined as a plug or an end section of the pipe.

Moment resistance

To calculate the moment resistance in the wall, the moment arm is essential. The large projectiles are all placed in horizontal position at a height of approximately 1 meter. Therefore, the moment arm is considered as the same. The moment force is given by *Eq. 9.16*.

$$M_{arm} = F \cdot l \quad \text{Eq. 9.16}$$

Where M_{arm} is the moment force and l the height of impact. Further, the deflection in the wall is given by *Eq. 9.17*.

$$f = \frac{F}{EI} \cdot \frac{l^3}{3} \quad \text{Eq. 9.17}$$

Here f is the deflection in the wall and I the moment of inertia. The moment of inertia is dependent on the shape of the wall.

Eq. 9.18 calculates the angle of the deflected wall at the area of impact.

$$A_F = \frac{1}{6} \frac{F^2 l^3}{EI} \quad \text{Eq. 9.18}$$

Where A_F is the angle of the deformed wall at impact.

The calculations do not consider buckling and walls are assumed to be fixed to the floor.

Axial resistance

For axial forces in the support, there is friction force from the weight of the wall, friction force from the fastening bolt and shear forces in the bolt. Friction coefficient is approx. 0.6. The axial force acting on the wall is expressed by Eq. 9.19.

$$A_x = F \quad \text{Eq. 9.19}$$

Where A_x is the axial force of the wall. The axial resistance of the wall is defined as Eq. 9.20.

$$A_r = F_{S,Bolt} + F_N + F_{N,Bolt} \quad \text{Eq. 9.20}$$

Here, A_r is the axial resistance of the wall, $F_{S,Bolt}$ the shear strength in the bolts defined in Eq., F_N is the gravitational force and $F_{N,Bolt}$ is the fastening force from the bolts. The gravitational force is expressed in Eq. 9.21.

$$F_N = m_w \cdot g \cdot \mu_f \quad \text{Eq. 9.21}$$

Where m_w is the mass of the wall and μ_f is the coefficient for friction between the wall and the floor. Further, the fastening force from the bolts is expressed in Eq. 9.22.

$$F_{N,Bolt} = \frac{2\pi \cdot G}{t_i} \mu_f \quad \text{Eq. 9.22}$$

Here G is the fastening torque and t_i is the thread incline. No friction force is considered during the fastening.

9.1.2 Concrete barrier

The most commonly used material for safety walls is reinforced concrete. This is concrete filled with steel bars as shown in *Figure 22*. Reinforced concrete has good compressive strength, have low cost on both raw material and production as well as it allows for large plastic deformation. Drawbacks are low shear and tensile strength, variation in concrete mixture and uncertainty in the material properties of the reinforcement.

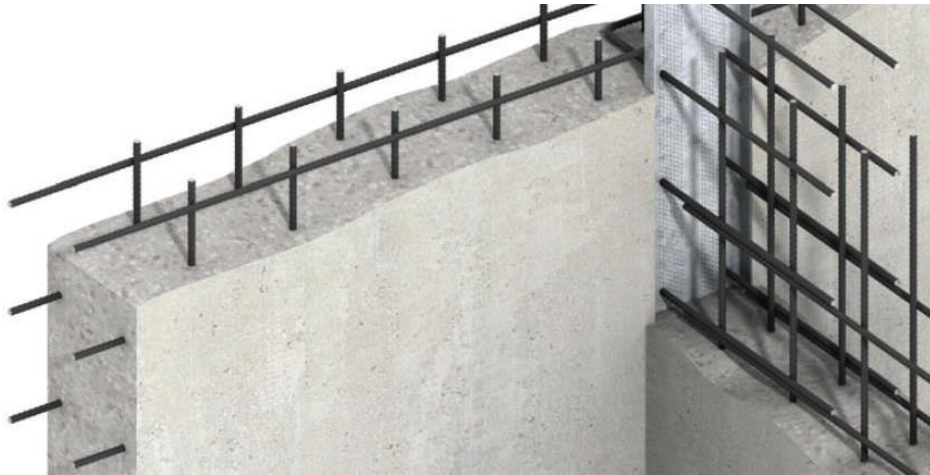


Figure 22 Reinforced concrete

The strength of the concrete is mainly decided by the concrete mixture and the amount of reinforcement. For normal reinforced concrete a compressive strength of 80 MPa is manageable. If the strength is insufficient, Ultra-High Performance Concrete can give compressive strength up to 200 MPa. The shear and tensile strength in RC is for the most part dependent on the reinforcement. The steel used in reinforcement should have high relative strength, high toleration of tensile strength and a good bond to the concrete.

The concrete has the same deformation as the reinforcement. The concrete and the reinforced steel also have linear elastic properties, which means Hooke's law applies (*Eq. 9.23* and *Eq. 9.24*)

$$\sigma_c = E_c \cdot \varepsilon \quad \text{Eq. 9.23}$$

$$\sigma_s = E_s \cdot \varepsilon \quad \text{Eq. 9.24}$$

Where σ_c is the concrete stress, E_c the elasticity modulus of concrete and ε is the strain. Further, σ_s is the steel stress and E_s the elasticity modulus of the reinforcement.

It is important to have equilibrium between the concrete and reinforcement. Therefore, the load is divided over both the concrete and reinforcement (Eq. 9.25).

$$F = E_c \cdot \varepsilon (A_c - A'_s) + E_s \cdot \varepsilon \cdot A'_s \quad \text{Eq. 9.25}$$

Here F is the load acting on the wall, A_c is the cross sectional area of concrete and A'_s the cross sectional area of the reinforcement. From Eq. 9.26, Eq. 9.27 and Eq. 9.28, we can find the joint strain in both the concrete and the reinforcement:

$$\varepsilon = \frac{F}{E_c \cdot (A_c - A'_s) + E_s \cdot A'_s} \quad \text{Eq. 9.26}$$

$$A_c = t \cdot b' \quad \text{Eq. 9.27}$$

$$A_s = n \cdot \frac{\pi \cdot d_s^2}{4} \quad \text{Eq. 9.28}$$

Where t is the wall thickness and b' is

To calculate the shear strength of the wall Eq. 9.29 is used.

$$\tau = \frac{V}{z \cdot b} \quad \text{Eq. 9.29}$$

Outer dimensioned moment M_{Ed} equal to M_{Rd} . $K = 0,177$.

The moment resistance in the wall is expressed by Eq. 9.30.

$$M_{Rd} = K \cdot f_{cd} \cdot b \cdot d^2 = M_{Ed} \quad \text{Eq. 9.30}$$

Where K is wall thickness, f_{cd} maximum stress, b width of the concrete wall and d the thickness of the wall.

Shear capacity of the wall is given by Eq. 9.32.

$$V = \frac{I \cdot b}{S} \cdot \sqrt{f_{ctd}^2 + \alpha_1 \cdot \sigma_{cp} \cdot f_{ctd}} \quad \text{Eq. 9.32}$$

Here I is second moment of area, S is static moment of cross-section above center of gravity calculated around center of gravity and f_{ctd} is the dimensioned tensile strength. The compressive stress on the concrete is given by Eq. 9.33.

$$\sigma_{cp} = N_{ed}/A_c < 0.2f_{cd} \quad \text{Eq. 9.33}$$

Rupture is further given as Eq. 9.34:

$$V_{rupture} = z \cdot b \sqrt{f_{ctd}^2 + \sigma_{cp} \cdot f_{ctd}} \quad \text{Eq. 9.34}$$

Axial resistance

The calculation of axial resistance in the wall is calculated the same way as in Ch. 9.1.1.

9.1.3 Composite barrier

Composite is often the combination of steel and concrete in the barrier. By combining the two, the advantages of both could be utilized. The steel could add to the shear and tensile strength of the concrete while the concrete lowers the coefficient of restitution and increase the time interval of an impact. The steel can increase the shear and tensile strength that the reinforcement supplies the wall.

When a steel plate is hit with a small, high velocity, projectile, the plate will experience local deformation, and the strength of the whole plate is not utilized. With a composite barrier consisting of concrete and a steel plate, the concrete will experience *scabbing* and give a larger contact area against the steel plate. This will lead to larger deformation and more energy is absorbed. The projectile will also have lower velocity, which also gives a more global effect on the steel plate.

Another composite material which may give the desired qualities is fiber-reinforced concrete. As the *Figure 23* show, the material contains of short fibers, which is uniformly distributed and randomly oriented. The fibers usually make between 0.3 and 2.5 percent of the volume in plain concrete. Fibers are added to the concrete to improve the structural properties, tensile strength and ductility.



Figure 23 Fiber-reinforced concrete

The compressive strength of concrete has large influence to the safety effect of the walls. The penetration factor. Shear strength, tensile strength, amount of reinforcement (armoring). Type of reinforcement.

9.2 Fixed safety walls

The new testing area is set up with four testing areas as seen in *Figure 24*. For illustration purpose a pipe is placed in each stall. There should be a fixed wall separating each of the testing stalls. The length of these walls vary to allow for testing with different pipe lengths. The reason for the design of the stalls, is to easily operate the pipes and install the testing equipment.

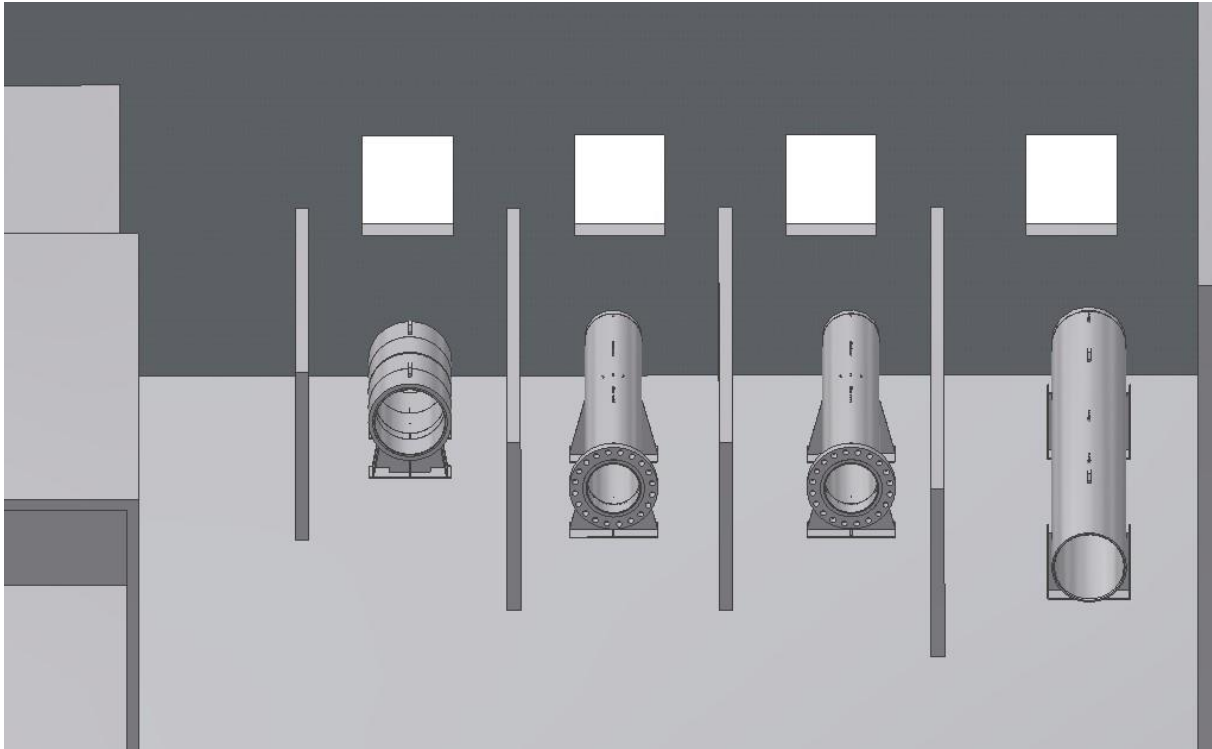


Figure 24 Model of the testing area

For practical reasons these walls will be made of concrete. This is because of production cost and properties of the material. According to T.D. Williamson's regulations, a fixed concrete safety wall is required to be minimum 220 mm thick. The design is based on this requirement. Further, the walls should have steel reinforcement which has high relative strength, high toleration of tensile strength and a good bonding with the concrete.

Table 20 give an overview of the properties of the partition walls between the different testing stalls

Table 20 Properties of fixed safety walls

	Symbol	Value
Wall thickness [m]	t	0.220
Compressive strength [MPa]	σ_c	80
Tensile strength [MPa]	σ_t	3
Compressibility water [1/Pa]	C	$4.55 \cdot 10^{-10}$
Young's modulus [GPa]	E	206

9.2.1 Penetration of fixed safety walls

From these specifications it is possible to calculate penetration as well as the possibility for perforation and scabbing. *Table 21* give different types of small, high velocity projectiles, which are used in the calculations. The mass and diameters are values to give a representation of different small projectiles.

Table 21 Properties of small projectiles

	Mass [kg]	Diameter [m]	Velocity [m/s]	
Projectile 1	0.1	0.01	2980	3827
Projectile 2	0.5	0.03	1333	1711
Projectile 3	1.0	0.08	943	1210
Projectile 4	2.0	0.14	666	856
Projectile 5	5.0	0.20	422	541
Projectile 6	10.0	0.30	298	383

Table 22 give the estimated penetration of the walls. Since the results is given without dimension as $\frac{x}{D}$, we have to find the penetration depth x . The analytical formula gives similar results as the empirical formulas for the larger projectiles. *Projectile 1* and *Projectile 2* have differ more from the other formulas. This is probably because the large projectile velocity is far outside the range of the formulas area of application.

Table 22 Penetration results of fixed safety walls

x/D :	Beth		Ace		NDRC		Bernard		Adeli & Amin		Hughes		Forrestal		Analytical	
Projectile 1	166.8	242.5	166.1	241.4	347.1	543.9	172.7	221.8	-	-	498.5	779.6	121.7	140.1	270.6	283.9
Projectile 2	12.1	17.4	12.1	17.4	17.8	27.3	14.3	18.4	-	-	28.8	43.8	11.5	14.5	26.6	29.0
Projectile 3	1.3	1.7	1.4	1.8	2.0	2.6	1.1	1.4	1.6	1.5	3.0	4.2	0.3	0.6	1.6	1.8
Projectile 4	0.6	0.7	0.7	0.8	1.2	1.3	0.3	0.4	0.5	0.7	1.1	1.4	-	-	1.8*	0.8
Projectile 5	0.6	0.5	0.6	0.7	1.1	1.1	0.2	0.2	0.2	0.3	0.7	0.8	-	-	0.9*	1.2*
Projectile 6	0.4	0.4	0.5	0.6	1.0	1.0	0.1	0.1	0.1	0.1	0.5	0.5	-	-	0.4*	0.5*

*Had to use *Eq.* for calculation

Table 23 shows the expected penetration depth of the projectile. Since the safety wall thickness will be 0.220 m, both *Projectile 1* and *Projectile 2* will probably penetrate the wall. Unfortunately, some of the calculations had to be performed with another formula, which gave higher penetration depth. The formula was not as complex which make the validity of the results uncertain.

Table 23 Penetration depth on fixed safety walls from the analytical model

	x [m]	
Projectile 1	2.706	2.839
Projectile 2	0.797	0.871
Projectile 3	0.124	0.145
Projectile 4	0.259*	0.106
Projectile 5	0.181*	0.232*
Projectile 6	0.121*	0.155*

*The validity of the result may probably be incorrect since *Eq.* was used in the calculation

Since the penetration depth of *Projectile 1* of such size, perforation is almost a certainty. In Table 24 the calculations were conducted with high strength concrete. The penetration is still well over 2 meter. The walls resistance against penetration has been increased, but not of any significance. Therefore, the use of high strength concrete is not necessary.

Table 24 Penetration depth with high strength concrete

	x [m]	
Projectile 1	2.595	2.728
Projectile 2	0.735	0.809
Projectile 3	0.107	0.128
Projectile 4	0.210*	0.100
Projectile 5	0.147*	0.189*
Projectile 6	0.098*	0.126*

*The validity of the result may probably be incorrect since *Eq.* was used in the calculation

9.2.2 Perforation of fixed Safety walls

With the same properties in the wall as during the penetration, the perforation is calculated for the projectiles with largest penetration. For the projectiles, which do not penetrate, the critical velocity is stated. Because of the placement of the pipes, the possible projectiles will only come from the pipe itself. These pipes are already approved for a higher working pressure than the testing pressure conducted at T.D. Williamson. This makes the probability of a pipe burst or collapse quite small. Still, if a hazard involving the pipe lead to injury, it is necessary to show calculations regarding wall strength.

Table 25 shows the perforation results from different formulas in Ch. 6. All of the perforation formulas are based on empirical results. The results show that *Projectile 1* and *Projectile 2* is unrealistic high. Since the range for these formulas is the same as for the penetration, the projectiles is probably too far out of range. The rest of the projectiles show more reasonable results. The *Chang formula* has an especially steep growth compared to the other formulas.

Table 25 Perforation results from empirical formulas for fixed safety walls

<i>h/D</i> :	NDRC		Chang		Adeli & Amin		Hughes	
Projectile 1	-	-	3979	4800	-	-	789.0	1233
Projectile 2	-	-	312.2	376.4	-	-	46.92	70.55
Projectile 3	3.522	3.416	29.32	35.35	2.384	2.979	6.123	8.106
Projectile 4	2.834	2.991	7.886	9.519	1.232	1.433	3.126	3.653
Projectile 5	2.667	2.728	3.630	4.374	1.021	1.094	2.487	2.727
Projectile 6	2.595	2.616	1.435	1.732	0.940	0.963	1.667	1.955

Table 26 shows the thickness of wall which gives perforation. According to these results, almost all of the projectiles will perforate the wall. The perforation thickness also increases with the diameter of the projectile, which is unrealistic. Even if the formulas is outside of their range, they indicate that the wall will be partly or completely perforated by the projectiles.

Table 26 Perforation thickness for fixed safety walls

<i>h</i> [m]	NDRC		Chang		Adeli & Amin		Hughes	
Projectile 1	-	-	39.79	48.00	-	-	7.890	12.33
Projectile 2	-	-	9.365	11.29	-	-	1.408	2.116
Projectile 3	0.282	0.273	2.346	2.828	0.191	0.238	0.490	0.649
Projectile 4	0.397	0.419	1.104	1.333	0.173	0.201	0.438	0.511
Projectile 5	0.533	0.546	0.726	0.875	0.204	0.219	0.497	0.545
Projectile 6	0.779	0.785	0.431	0.520	0.282	0.289	0.500	0.155

When comparing the penetration and perforation results, it shows that the calculations of perforation is more conservative and give larger length than that of penetration. This may be due to the wall weakening from cracking and brittle fracture. The projectile has a large velocity which will cause the wall to act brittle when absorbing the kinetic energy.

9.3 Existing Safety walls

TDW Offshore Services already have four portable safety walls. The thesis will analyze and calculate if these are sufficient as protection against the hazards mentioned earlier in the thesis. The walls are made of concrete and was made by Aarbakke AS. Unfortunately, there is no data sheet on the walls, which means the strength of the walls are uncertain. The concrete is reinforced with 300 kg of steel, but there is no mention of the reinforcement method. This gives uncertainties to the strength and ductility of the concrete. *Figure 25* shows the existing safety walls. It is possible to bolt them to the ground to increase the resistance against shear forces and to join multiple walls together.

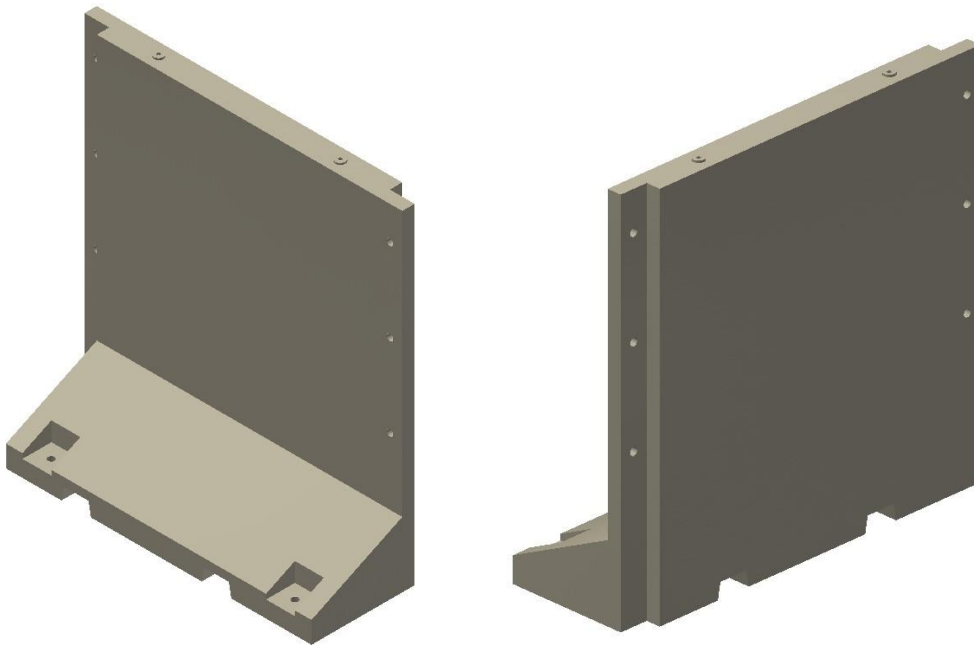


Figure 25 Existing safety walls

Table 27 give an overview of the properties of the safety walls and approximations made concerning unknown values. There is some uncertainty to the compressive and tensile strength of the walls.

Table 27 Properties of existing safety walls

	Symbol	Value
Wall thickness [m]	t	0.15
Compressive strength [MPa]	σ_c	50
Tensile strength [MPa]	σ_t	2.33
Weight [kg]	m_{sf}	1900
Density [kg/m ³]	ρ	2400
Young's modulus [GPa]	E	206

9.3.1 Penetration

From these specifications it is possible to calculate penetration as well as the possibility for perforation and scabbing. The same projectiles are used in the calculations as Table 28.

Table 28 Penetration results of existing safety walls

x/D :	Beth		Ace		NDRC		Bernard		Adeli & Amin		Hughes		Forrestal		Analytical	
Projectile 1	210.8	306.7	209.9	305.3	438.7	687.7	218.5	280.6	-	-	498.5	779.6	129.6	148.0	276.3	289.6
Projectile 2	15.2	21.9	15.2	21.9	22.3	34.3	18.1	23.3	-	-	28.8	43.8	12.8	15.9	27.6	30.1
Projectile 3	1.5	2.0	1.6	2.2	2.3	3.1	1.4	1.7	1.5	-	3.0	4.2	0.4	0.7	1.7	1.9
Projectile 4	0.6	0.8	0.8	0.9	1.3	1.4	0.4	0.5	0.7	1.1	1.1	1.4	-	-	0.7	0.8
Projectile 5	0.5	0.5	0.6	0.7	1.1	1.2	0.2	0.2	0.3	0.4	0.7	0.8	-	-	1.3*	1.2*
Projectile 6	0.4	0.4	0.6	0.6	1.0	1.1	0.1	0.1	0.1	0.2	0.5	0.5	-	-	0.4*	0.6*

*Had to use *Eq.* for calculation

Table 29 give a representation of the results from each of the projectile types given in Table 21.

Table 29 Penetration depth of existing safety walls based on analytic model

	x [m]	
Projectile 1	2.763	2.896
Projectile 2	0.829	0.903
Projectile 3	0.133	0.154
Projectile 4	0.101	0.110
Projectile 5	0.202*	0.259*
Projectile 6	0.134*	0.173*

*The validity of the result may probably be incorrect since *Eq.* was used in the calculation

As we can see from the results in Table 29, many of the projectiles will perforate the wall.

With the same specifications as during the penetration, the perforation is calculated for the projectiles with largest penetration. For the projectiles, which do not penetrate, the critical velocity is stated.

Table 30 give a collection on the perforating results of the existing safety walls for the different projectiles.

Table 30 Perforation results existing safety walls

h/D :	NDRC		Chang		Adeli & Amin		Hughes	
Projectile 1	-	-	5032	6071	-	-	789.0	1233
Projectile 2	-	-	394.8	476.1	-	-	46.92	70.55
Projectile 3	3.535	3.016	37.09	44.72	2.946	3.342	6.122	8.106
Projectile 4	2.907	3.105	9.975	12.04	1.417	1.708	3.126	3.653
Projectile 5	2.696	2.772	4.592	5.533	1.089	1.203	2.487	2.727
Projectile 6	2.605	2.630	1.815	2.191	0.961	0.996	1.667	1.955

Further, the perforation thickness of the existing safety walls is given in *Table 31*. Some of the results are high and unrealistic, but the kinetic energy of the projectiles as well as wall strength is outside the range of the formulas. This makes the results unreliable for use in calculation of wall thickness.

Table 31 Perforation thickness existing safety walls

h [m]	NDRC		Chang		Adeli & Amin		Hughes	
Projectile 1	-	-	50.32	60.71	-	-	7.890	12.33
Projectile 2	-	-	11.85	14.28	-	-	1.408	2.116
Projectile 3	0.282	0.241	2.967	3.577	0.236	0.267	0.490	0.649
Projectile 4	0.407	0.435	1.396	1.686	0.198	0.241	0.438	0.511
Projectile 5	0.539	0.554	0.918	1.107	0.218	0.241	0.497	0.545
Projectile 6	0.781	0.790	0.545	0.657	0.288	0.299	0.500	0.586

9.3.2 Scabbing

Scabbing is when a section of the wall is released from the wall due to perforation. *Figure 26* shows the other side of the same wall as shown earlier. At the point of exit a larger section is missing compared to the point of impact. As scabbing weakens the walls integrity, it is important to prevent scabbing from occurring.



Figure 26 Scabbing of safety wall

Due to the specifications of projectiles during testing and the strength of the wall is far outside the range of the formulas, the thesis

9.3.3 Shear forces

The safety walls ability to withstand shear forces is determined locally by the reinforcement. Both the strength of the reinforcement and the cross-section decides the shear strength of a concrete wall.

Still, the walls have to withstand the shear forces on globally as well. In other words, the walls should not be tipped over by shear forces. The walls have a quite high center of gravity, which impairs the ability to handle large shear forces. *Figure 27* show the necessary force to tip over the wall.

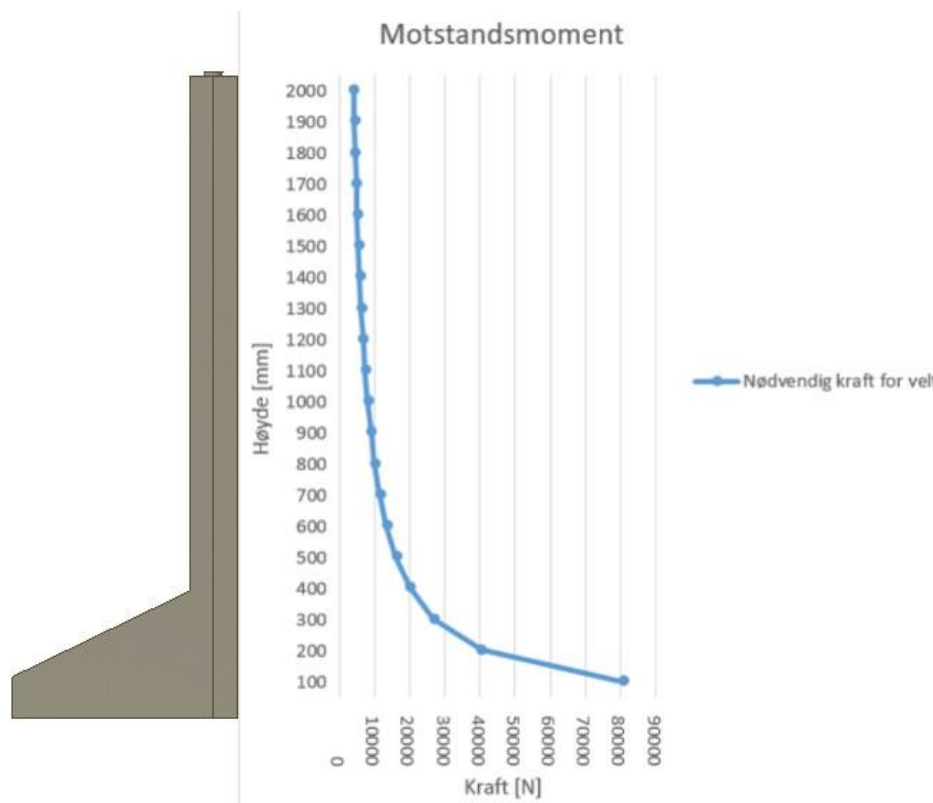


Figure 27 Moment forces existing safety walls

Table 32 give a representation of a discharge by an end section or a plug.

Table 32 Properties of large projectiles

	Mass [kg]	Diameter [m]	Velocity [m/s]
End section	400 – 900	0.741 – 1.153	47.1-40.3
Plug small	1300	0.741	26.1
Plug large	6000	1.153	15.6

9.4 Steel safety walls

A good option for safety walls are barriers made of steel. The walls will have high strength compared to density and give large shear strength compared to concrete. This gives less requirement to the thickness of the barrier. The principle for this design is a hollow frame which will give stiffness to the wall and a plate in the middle to absorb impacts as *Figure 28* shows.

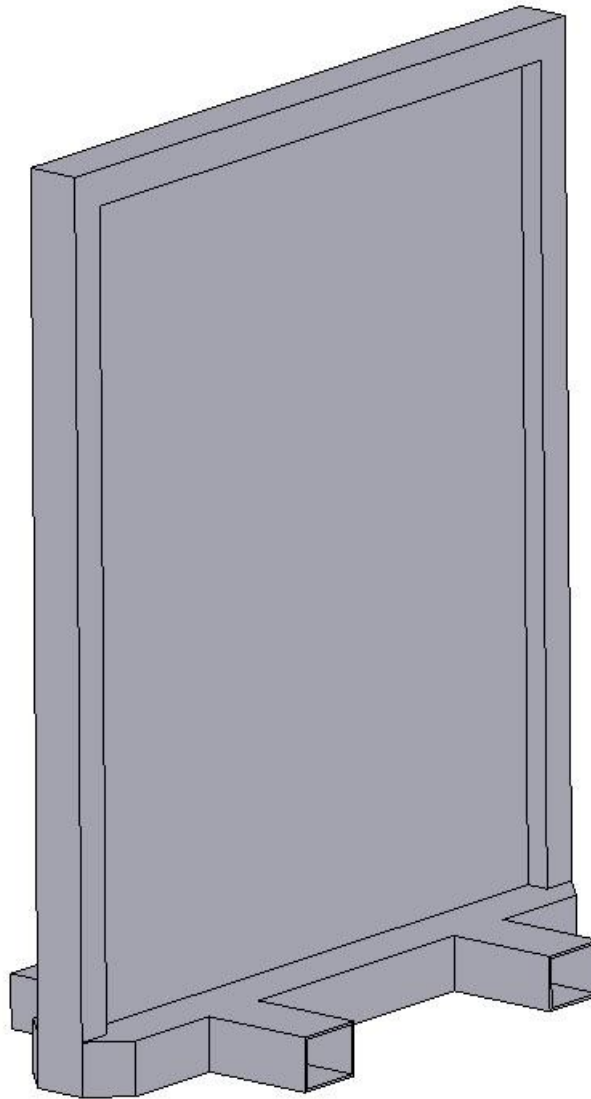


Figure 28 Steel barrier

If the impact mainly causes local damage to the wall depends on the size and velocity of the projectile. A large projectile will create a global deflection in the wall and more energy is absorbed through plastic deformation. A small projectile will create a more local deformation and the strength of the whole wall is not utilized. This will give a smaller area of deformation, which means a smaller area will be able to absorb the kinetic energy of the projectile.

9.4.1 Energy absorption during impact

When determining the walls ability to absorb energy from impacts, it was necessary to know the strain at fracture. The materials in consideration is s355, 316L and 304L with an elongation of 18%, 50% and 60-70%, respectively. The calculations have been performed for wall thickness of 0.020 and 0.025 meter. Due to large impulse force, the wall will be subjected to a local deformation. The cross-sectional area of the deformation is assumed to be twice that of the projectile.

Table 33 and *Table 34* give the results of energy absorption during impact for the different projectiles.

Table 33 Energy absorption with wall thickness 0.02 m

$t = 0.020$ m	S355 [J]	AISI 316L [J]	AISI 304L [J]
Projectile 1	3532.6	114605	149562
Projectile 2	10598	343816	448685
Projectile 3	28261	916842	1196494
Projectile 4	49456	1604474	2093865
Projectile 5	70652	2292106	2991236
Projectile 6	105978	3438159	4486854

Table 34 Energy absorption with wall thickness 0.025 m

$t = 0.025$ m	S355 [J]	AISI 316L [J]	AISI 304L [J]
Projectile 1	4415.7	143257	186952
Projectile 2	13247	429770	560857
Projectile 3	35326	1146053	1495618
Projectile 4	61820	2005593	2617332
Projectile 5	88315	2865133	3739045
Projectile 6	132472	4297699	5608568

9.4.2 Effect of large projectiles on steel wall

A large projectile will affect the wall on a global scale. To stop or decelerate the projectile, it is necessary with moment resistance in the wall. To simplify the calculations, the moment resistance was based on the frame of the wall. The cross-section of the frame is shown by *Figure 29*. By using *Eq. 9.17* for deflection and *Eq. 9.35* for moment of inertia, the maximum deflection for the given forces could be estimated.

$$I = \frac{B \cdot H^3 - b \cdot h^3}{12}$$

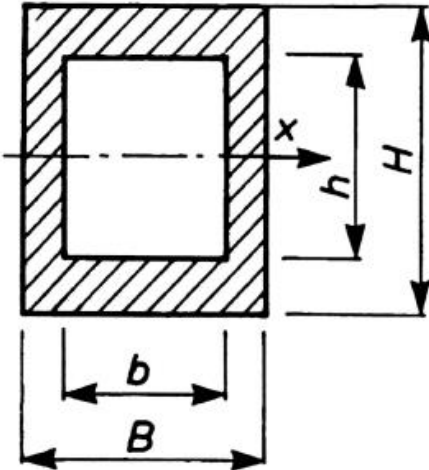


Figure 29 Cross-section of frame

Table 35 show the frame properties from *fig*:

Table 35 Frame properties for steel wall

	Frame properties [m]
B	0.100
b	0.080
H	0.150
h	0.110

Table 36 shows the forces from large projectiles, frame specifications as well as corresponding deflection in the wall.

Table 36 Forces acting on wall

	Approx. Δt^*	Shear force [N]
Small end section	0.0085	2217659
Small plug	0.0153	2221079
Large end section	0.0099	3666874
Large plug	0.0256	3659766

*Time period for distance 0.2 meter

Further, *Table 37* shows the calculated moment of inertia and deflection of the wall.

Table 37 Properties wall

	Symbol:	Value
E-module [GPa]	E	206
Moment of inertia [m ⁴]	I	$1.925 \cdot 10^{-5}$
Length [m]	l	1.0
Acting force [N]	F	3666874
Deformation [m]	f	0.308

From hand calculations, the expected deformation in worst case will be 0.308 m. Compared to analysis performed in Autodesk Inventor (*Figure 30*), the deformation at the same height is less (approx. 0.126 m). This is most likely due to the simplification in the hand calculations. The thesis does not calculate for buckling of the frame.

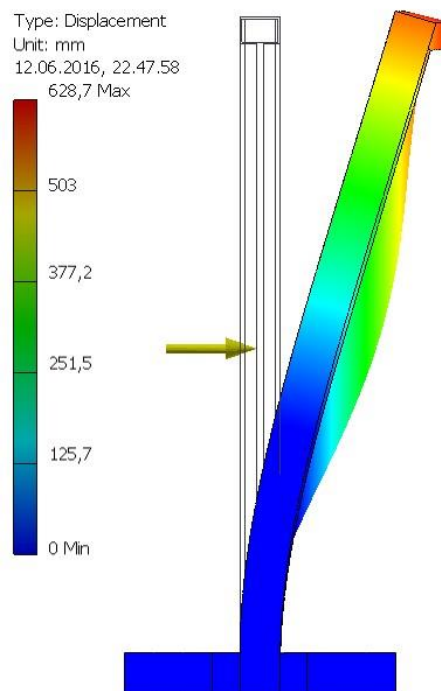


Figure 30 Analysis of deflection of steel wall

9.4.3 Resistance to shear forces

The walls ability to withstand axial forces is dependent on friction force and strength of fasteners. The friction coefficient between concrete and steel is approximately 0.6 under static conditions. The friction force is then the normal force from both the weight of the wall as well as the fastening bolts. For the calculation, Ø40 bolts with grade 8.8 is considered. Using *Eq.* for shear strength in bolts as well as *Eq.*, which gives the normal force from weight of wall and fastening of bolts. The bolts are fastened with a torque of 100 Nm and pitch of 4 mm. The results from the calculations is given in *Table 38*.

Table 38 Steel walls resistance to shear force

	Axial force [N]
Friction force wall	8240
Shear strength bolts	3015928
Friction force bolts	376991*
Total shear resistance	3401160

*The torque is considered without friction forces.

The shear forces from the different projectiles is given in *Table 39*. The results show that the different sections of the pipe have the same kinetic energy. The wall would probably not be able to contain either of the projectiles, since the bolts will be exposed to moment forces which will weaken the shear capacity. Still, the walls will greatly reduce the energy in the projectile, and thereby lowering the severity of the hazard.

Table 39 Force from large projectiles

	Approx. Δt^*	Shear force [N]
Small end section	0.0085	2217659
Small plug	0.0153	2221079
Large end section	0.0099	3666874
Large plug	0.0256	3659766

*Time period for distance 0.2 meter

Figure 31 illustrate the wall with axial and applied forces.

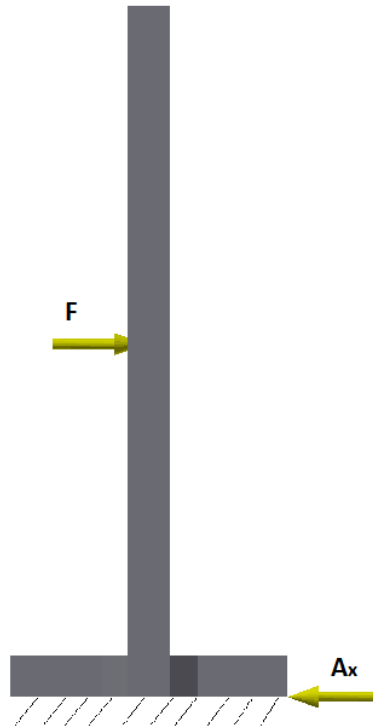


Figure 31 Shear forces

According to these calculations will the steel wall provide a good protection during pressure testing. The area which gave the least protection was small projectiles. The high velocity and small diameter creates a local deformation which prevents the utilization of the whole wall.

9.5 Composite safety walls

The composite walls will be in this case the combination of steel and reinforced concrete. This is to increase the tensile and shear strength of the wall. With concrete's ability to absorb energy through plastic deformation a combination of steel and reinforced concrete give a desirable product. For new composite walls, the thesis recommends a similar shape to the existing safety walls with a steel plate attached to increase the shear strength of the wall.

9.6 Existing safety walls 1

An option may be to apply a steel plate behind the existing safety walls to increase the strength of the wall. To fix the plate to the wall it will be necessary with bolts as shown in *Figure 32*.

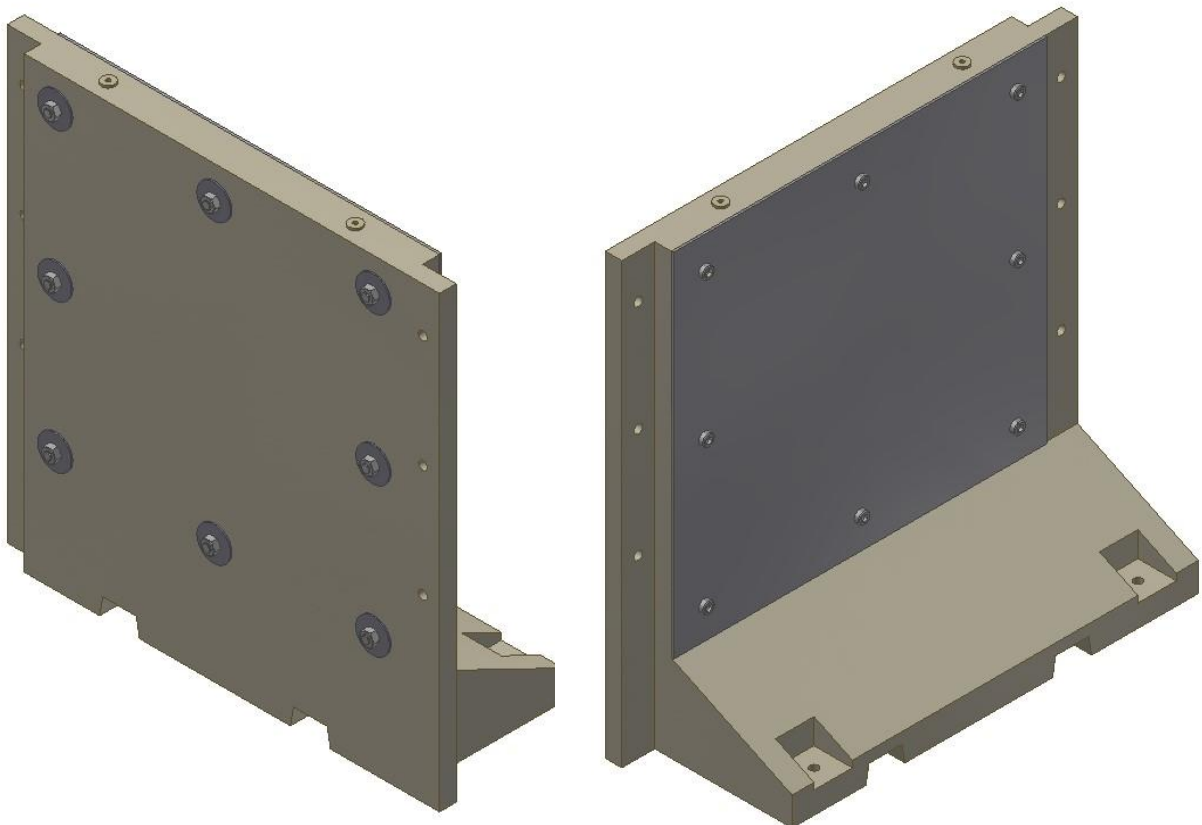


Figure 32 Composite safety walls with bolted steel plate

A problem with this solution to the existing safety walls is that there are no drawings or details regarding the location of the reinforcement. The holes will therefore weaken the strength of the wall if the reinforcement is damaged. The location of the bolts gives the plate room for larger deformation and can therefore absorb more kinetic force from a projectile.

A way to locate the reinforcement could be a non-destructive test of the wall. With the right test, it will be possible to locate the steel bars inside the wall.

9.7 Existing safety walls 2

Figure 33, shows the existing safety walls with a steel plate that covers the wall. This method does not require fastening, and have the same properties as the other option. The production cost might be higher, due to more complex shape and higher requirement on tolerances.

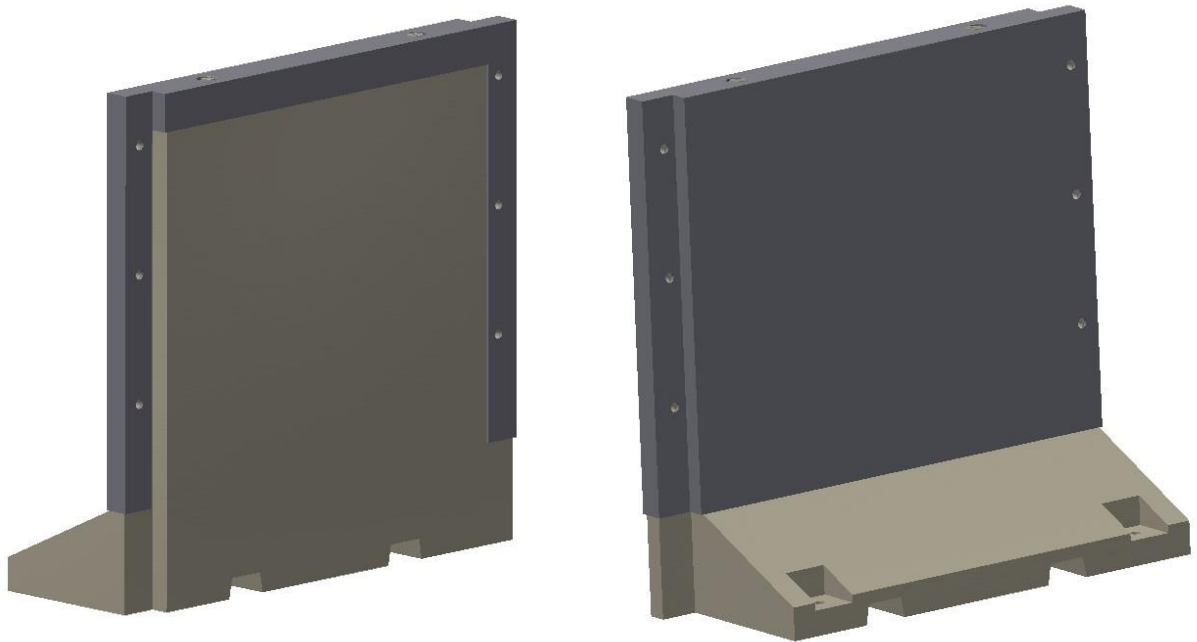


Figure 33 Existing safety walls with welded plate

10 Discussion of design

When the safety level of the tests should be determined, there is a lot of factors involved. Firstly, the energy inside the pressurized vessel is the main deciding factor for the extent of the hazard. The test performed showed that the *Baker formula* together with the elastic energy of the material gave the best representation of the energy inside the test.

For further calculations, a range of small projectiles was used as basis. The projectiles were all small and varied in weight, diameter and velocity. These were used when calculating penetration depth into concrete. An analytical model was the best fit, and gave an indication regarding how sufficient the barrier was as protection. The most critical projectiles were the ones with smallest diameter and highest velocity. Due to large potential energy inside the pressure vessel, the velocity of the smaller projectiles was estimated to have a velocity of many times the speed of sound.

As an alternative to safety walls of concrete, the design of steel walls has been developed. A problem with steel walls are high *impulse force* at impact, the possibility of *bounce-back* and higher cost both in materials but also in production. Advantages with a steel wall is high strength compared to density and large shear strength. A small projectile impact will create a local deformation. This is due to large impulse forces and moment of inertia. To calculate the energy absorbed by the wall, it was necessary to estimate the size of the local deformation. Another deciding factor for the absorbed energy is the toughness of the material.

Based on calculations, the steel walls will also not able to contain the energy of a discharged projectile from the largest tests. The velocity together with small diameter makes the deformation in the wall quite local for both the concrete and steel walls. Therefore, the strength of the wall is not fully utilized. Based on the calculations on penetration, there should be at least two layers of safety walls between the test vessel and operators. This include the both the portable safety walls, but also the fixed safety wall. In other words, the test area next to the largest tests should be closed off while conducting the most hazardous tests.

To increase the strength of the existing walls, a steel plate behind the wall will strengthen the shear strength of the wall, prevent scabbing and give room for larger deformation. This is a good alternative, as it utilizes the advantages from both materials. The thesis has given two suggestions on how to quite easily attach such a plate.

The first option is to attach the plate with bolts through the concrete. Although, if the reinforcement is damaged, this will decrease the strength of the wall. To prevent this, a non-destructive test like ultrasonic or x-ray might locate the reinforcement. When making the holes in the wall it is important to avoid the reinforcement. For this option, it is important to use large washers to distribute the force from the bolts.

The second option is to weld a plate according to **Figure**. This way, the steel plate will provide its own fastening. This way, the integrity of the concrete wall will not be weakened. This option will however have larger material and production costs. This is because the design is more complex than in the first option.

To stop or decelerate larger projectiles like a plug or an end section, the wall need to be fixed to the floor and surrounding walls. The easiest fastening method is to use bolts between the safety walls and surrounding structures. Originally, the walls have low resistance against moment forces due to the relationship between height and cross-section. This is why it is necessary to fasten the safety walls to increase the resistance of moment in the wall.

The walls should be covered by a soft, deformable material to decrease the impulse force. This will also decrease the noise level on impact. *Proserv AS* recommended the use of 18-20 mm OSP-plate. To include the wooden plate in the calculations will be difficult since the toughness and elasticity of the plate is unknown.

For the calculations, the following assumptions have been made

- The end flanges in the pipes are assumed to be rigid
- The cylindrical body is free to expand in the radial and longitudinal direction of the pipe
- No vapor or gas pockets are present in the pressure vessel
- Energy losses due to friction, air resistance and leakage are neglected
- Constant Bulk Modulus of water

Figure 34 shows a model of the new testing area with the four existing safety walls. To be able to use all testing area efficiently in a safe way, it is necessary with more safety walls. It would be necessary to cover each testing stall with two walls. The stall furthest to the right should also have two layers of safety walls as well as a closed off zone to lower the risk to an acceptable level.

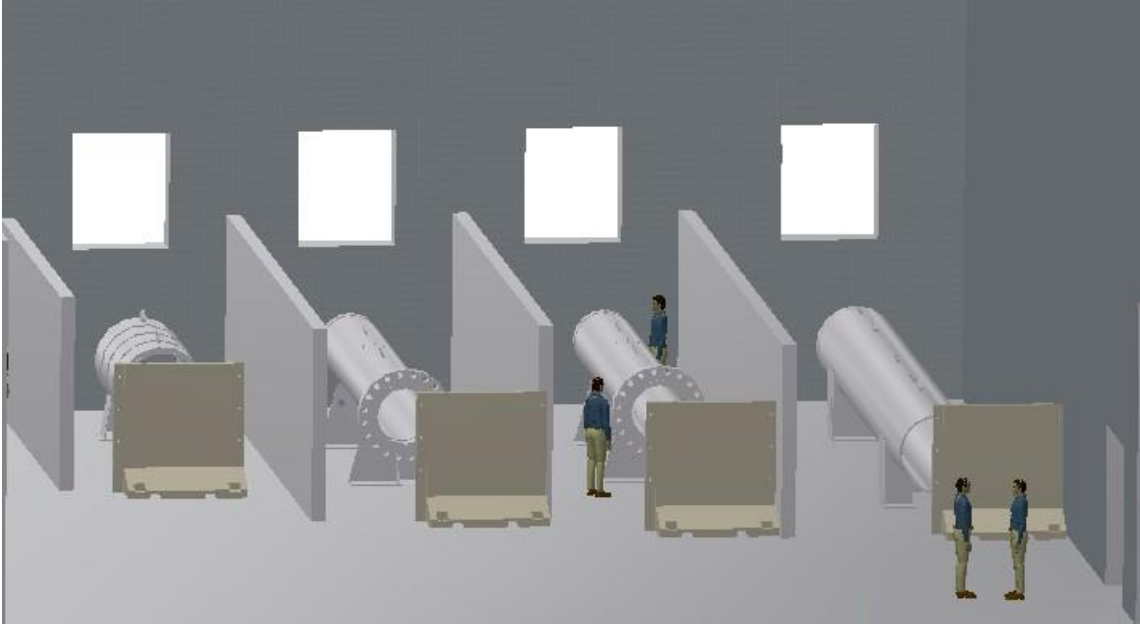


Figure 34 New testing area with existing safety walls

11 Conclusion & Further Work

11.1 Conclusion

The purpose of this thesis was to find optimal design for projectile and blast protection during pressure testing. Further, it was to evaluate the safety installments already in place and analyze the forces and risks involved in case of failure. According to the Norwegian regulations regarding safety in pressure testing a risk analysis is required for the operation and area as documentation. Thus, this thesis aims to give an assessment of the hazards involved in pressure testing and recommend measures to lower the risk to an acceptable level.

A part of the thesis was to conduct a risk analysis. By assessing the hazards identified in the thesis through calculations, the risk analysis was lowered to a safe level. Based on the results in the calculations, mediating measures have been suggested to reach a safety level which is as low as reasonable practicable.

To support the calculation, a projectile discharge test was conducted. The test showed that the *Baker formula* and the elastic energy in the pipe gave the best representation of the potential energy inside a pressurized vessel. In worst case scenario, a projectile from one of these tests will have a velocity many times the speed of sound. The magnitude of possible energy release in a pressure test, resulted in more parameters in the calculations. Important factors for determining the safety level are penetration, impulse force, the walls ability to absorb energy and to withstand shear and moment forces.

The calculations of penetration of the safety walls showed that the tests with largest potential energy will cause perforation. Also, the walls are not able to handle the moment forces of a larger projectile like a plug or end section of the pipe. Therefore, the test area should be protected by two layers of safety walls when conducting the most hazardous tests. This recommendation concerns the fixed safety walls as well. The testing stall next to the pressure test should be closed off during testing for the tests considered in this thesis.

To reinforce the existing safety walls, a steel plate should be attached behind the wall. This will increase the walls shear strength as well as the ability to absorb energy. To reduce sound and large impulse forces the use of 18-20 mm OSP-plate in front of the safety wall is recommended. The plate will absorb energy through plastic deformation and reduce the impulse force as well as reduce the bounce back. The plate will have no effect on the worst cases considered in this thesis.

In the new workshop there will be four testing stalls. As **Figure** shows, the walls are not big enough to cover the entire stall. Therefore, it is recommended to obtain more safety walls so the testing area can be utilized efficiently. The design which would give the best protection

is a wall of reinforced concrete based on existing safety walls with a steel plate attached. Preferable, this wall should have a compressive strength of 80 MPa or more.

It is important to protect the windows and other weak parts in the workshop from hazards. Preferably, a drawing of the area with specifications regarding the structure for calculation purposes. Important factors are the thickness of roof, walls and floor together with the material strength of the building material.

In the event of failure and discharge of a projectile, the safety walls will most likely be exposed to plastic deformation and even perforation. This will weaken the integrity of the wall and impair the walls protective ability. A visual inspection of the wall should be sufficient to determine the extent of damage on the wall. A water jet, a pressure wave or impact from the pressure hose will most likely not inflict any damage to the walls.

11.2 Recommendations for further work

The thesis has a wide theoretical range with many different subjects. Therefore, the thesis was not able to go into the depth of all theory. For further work, there is a few subjects that could be more thoroughly covered:

1. The safety distance from pressure wave with implanted safety barriers. How do the safety walls confine the pressure wave energy?
2. The *perforation* and *scabbing* formulas for concrete walls is quite old and a little outdated. They are mostly empirical, with a range mostly outside the scope of the projectiles in this thesis.
3. Calculation of residual velocity and energy in a projectile after perforation.
4. The effect of impulse force on a steel wall regarding energy absorption and local effect. Find how the impulse force changes the ductility of the material and how that affect the size of the deformation.
5. More extensive testing of pressure burst. Measurement of energy inside the pressure vessel with larger volume and pressure but also projectile impact test on safety walls.
6. Calculation of shear and moment resistance in concrete walls
7. A study of more suitable material for the safety walls.

12 References

- (1) Adeli, H. and Armin, M. (1985), Local Effects of Impactors on Concrete Structures. *Nuclear engineering and Design*. Vol. 88, pp. 301-317.
- (2) ANSI (January 2007), Pressure-Relieving and Depressuring Systems, *ANSI/API Standard 521*, 5th ed.
- (3) Aven, T. (2008), *Risk Analysis*. Chichester, West Sussex: John Wiley & Sons Ltd.
- (4) Baker, W.E. (1973), *Explosions in Air*, Austin, TX: Univ. of Austin Press.
- (5) Bernard, R.S. (1976), Empirical Analysis of Projectile Penetration in Rock. U.S. Army Waterways Experiment Station Paper AEWES-MP-S-77-16.
- (6) Beth, R.A., Concrete Penetration, NDRC Report No. A-319, OSRD Report No. 4856.
- (7) Chang, W.S. (1981), Impact of Solid Missiles on Concrete Barriers, *Journal of the Structural Division*, Vol. 107, No. ST2, pp. 257-271.
- (8) Chelapati, C.V., Kennedy, R.P. (1972), Probability Assessment of Aircraft Hazard for Nuclear Power Plants, *Nuclear Engineering and Design*, Vol. 19, pp. 333-364.
- (9) Coulson, J.M., Richardson, J.F. (1977), *Chemical Engineering* (SI ed.) Oxford, OX: Pergamon Press.
- (10) Cox, B.G., Saville, G. (1975), *High Pressure Safety Code*. High Pressure Technol. Ass., Imperial Coll., London.
- (11) Dean, J., Dunleavy, C.S., Brown, P.M., Clyne, T.W. (2009), Energy Absorption during Projectile Perforation of Thin Steel Plates and the Kinetic Energy of Ejected Fragments, *International Journal of Impact Engineering*, Vol. 36, No.10, pp. 1250-1258.
- (12) Fenner, R. T., Reddy, J.N. (1999), *Mechanics of Solids*, Boca Raton: CRC Press LLC.
- (13) Forrestal, M.J., Altman, B.S., Cargile, J.D., Hanchak, S.J. (1994), An empirical equation for penetration depth of ogive-nose projectiles into concrete targets. *Int. J. Impact Engng*, Vol. 15, No.5, pp. 395-405.
- (14) Forrestal, M.J., Frew, D.J., Hanchak, S.J., Brar, N.S. (1996), Penetration of grout and concrete targets with ogive-nose steel projectiles. *Int. J. Impact Engng*, Vol.

18, No.5, pp. 465-476.

- (15) Forskrift om håndtering av farlig stoff (2009), Ministry of Justice and Public Security, Norway.
- (16) Forskrift om trykkpåkjent utstyr (1999), Ministry of Justice and Public Security, Norway.
- (17) Güttler, C., Heißelmann, D., Blum, J. and Krijt, S. (2013), Normal Collisions of Spheres: A Literature Survey on Available Experiments, physics.class-ph: arXiv:1204.0001v2.
- (18) Hartvigsen, H., Lorentsen, R., Michelsen, K., Seljevoll, S. (2006), Verksted Håndboka 6th ed., Tromsø: Gyldendal.
- (19) Hormann, C. (2012, March, 13), Patch Functions Reference. Retrieved from <http://www.imagico.de/simpov/docu01.php>
- (20) Hughes, G. (1984), Hard Missile Impact on Reinforced Concrete. *Nuclear Engineering and Design*, Vol. 77, pp. 23-35.
- (21) Kim, O.V., Dunn, P.F. (2007) A Microsphere-Surface Impact Model for Implementation in Computational Fluid Dynamics, *Aerosol Science*, Vol. 38, pp. 532-549.
- (22) Kinney, G.F. and Graham, K.J. (1985). Explosive Shocks in Air, 2nd ed. New York: John Wiley & Sons Ltd.
- (23) Latif, Q.B.A.I, Rahman, I.A., Zaidi, A.M.A, Latif, K. (2012), Analytical Model for Critical Impact Energy Required to Penetrate Concrete Slab Impacted with Ogive Nose Hard Projectile, *IIUM Engineering congress 2012*, pp. 319-328.
- (24) Li, Q.M., Chen, X.W. (2003) Dimensionless formulae for penetration depth of concrete target impacted by a non-deformable projectile, *Int. J. Impact Eng.*, Vol. 28, No. 1, pp. 93-116.
- (25) Li, Q.M., Reid, S.R., Wen, H.M., Telford, A.R. (2005) Local impact effects of hard missiles on concrete targets, *Int. J. Impact Eng.*, Vol. 32, pp. 93-116.
- (26) Lewitt, E.H. (1952), Hydraulics, 9th ed. London: Pittman
- (27) Lifshitz, J. and Kolsky, H (1964). Some experiments on anelastic rebound. *Journal of the Mechanics and Physics of Solids*, Vol. 12, No. 1, pp. 35-43.

- (28) Mannan, S. (2005), *Lees' Loss Prevention in the Process Industries 3rd ed.* Oxford, Ox: Elsevier.
- (29) Paulsen, S.S. (2009), *Pressure Systems Stored-Energy Threshold Risk Analysis, PNNL Standards Based Management System.* Richland, WA: Pacific Northwest National Laboratory.
- (30) Protective Design, *Fundamentals of Protective Design (Non-Nuclear)*, (1965, July). Department of the Army Technical Manual TM5-855-1.
- (31) PSA. (2001) *Regulations Petroleum Safety Authority Norway.*
- (32) SINTEF (2003), *Handbook for Fire Calculations and Fire Risk*, Norwegian Fire Research Laboratory.
- (33) Sørensen, S.I. (2010), *Betongkonstruksjoner*, Trondheim: Tapir Akademisk Forlag.
- (34) Teland, J. A. (1998, January), *Review of Empirical Equations for Missile Impact Effects on Concrete*, Norwegian Defence Research Establishment, FFIVM/708/130.
- (35) Thornton, C., Ning, Z. (1998). A Theoretical Model for the Stick/Bounce Behaviour of Adhesive, Elastic-Plastic Spheres, *Powder Technology*, Vol. 99, No. 2, pp. 154-162.
- (36) WorkSafeBC (2009), *Young Worker Dies after Pressure Testing Oil Field Piping, Hazard Alert*, BC.

Attachments (Appendix)

APPENDIX A: RISK ANALYSIS	88
APPENDIX B: WATER TABLE – THERMODYNAMICS	89
APPENDIX C: SIMPLE DERIVATIONS	91
APPENDIX D: HYDROSTATIC TEST	93
TEST PROCEDURE.....	93
DRAWING PROJECTILE	97
DRAWING OF TEST ASSEMBLY.....	98
OUTLAY OF THE TESTING AREA FOR PROJECTILE DISCHARGE.....	99
PROPERTIES BRASS.....	101
DATALOG FROM TEST.....	102
APPENDIX E: EXISTING SAFETY WALLS	103
APPENDIX F: PRE-STUDY REPORT.....	104

Appendix A: Risk Analysis

Failure Mode: Hydrostatic pressure testing																																									
No.	Description of Operation Mode	Scenario	Hazard	Situation	Consequence	Attendees:			Cause	Risk reducing Measures in place	Proposed actions	After Risk Red		Comment																											
						Initial Risk	P	Risk				S	P		Risk																										
1	Failure of pipe	1.1	Pressure wave	Rapid release of energy	Bursting ear drums	5	3	2	6	Pipe damaged or overpressure	Safety walls, inspection of pipe, measuring device to control pressure	Close down danger area	1	2	2																										
																1.2	Water jet	High velocity water jet	High velocity stream hits body	3	2	6	Pipe damaged, overpressure or bleed out pressure. Not wearing PPE	Safety walls, inspection of pipe, measuring device to control pressure, remove controlled bleed out	Close down danger area and Multiple safety walls	2	2	4													
																													1.3	Discharge of fragments	Release of high velocity fragments	Severe injury or fatality from blunt objects	5	2	10	Pipe damaged or overpressure	Safety walls, inspection of pipe, measuring device to control pressure	Close down danger area and Multiple safety walls	2	2	4
2	Failure of plug	2.1	Pressure wave	Rapid release of energy	Bursting ear drums	3	2	6	Plug damaged, overpressure or fault in plug	Safety walls, inspection of plug and Measuring device to control pressure	Close down danger area	1	2	2																											
															2.2	Water jet	High velocity water jet	High pressure stream hits body	3	2	6	Plug damaged, overpressure or fault in plug. Not wearing PPE	Safety walls, inspection of plug and Measuring device to control pressure	Close down danger area and Multiple safety walls	2	2	4														
																												2.3	Discharge of fragments	Release of high velocity fragments	Severe injury or fatality from blunt objects	5	2	10	Plug damaged, overpressure or fault in plug	Safety walls, inspection of plug and Measuring device to control pressure	Close down danger area and Multiple safety walls	2	2	4	
																																									2.4
3	Failure of hose	3.1.	Hose release	High velocity object	Straining of body	3	3	9	Hose damaged or overpressurized. No wearing PPE	Safety wire or pressure strap on hoas	Close down danger area and Multiple safety walls	1	3	3																											
															4	Movement of test vessel due to collapse	4.1	Make the rig reducing measures less effective	increase consequence	injury or fatality	5	2	10	A large amount of energy is released which can cause movement in test fluid to this.	Fits to floor or legs by use of straps	2	1	2													
5	Other	5.1	Dive					0	Steps cannot be followed in the order written in the procedure.		Re-use procedure to match best practice			0																											
															5.2																										

Appendix B: Water table – Thermodynamics

Compressed Liquid Water

Temp. (°C)	v (m ³ /kg)	u (kJ/kg)	h (kJ/kg)	s (kJ/kg-K)	v (m ³ /kg)	u (kJ/kg)	h (kJ/kg)	s (kJ/kg-K)
500 kPa (151.86°C)								
Sat.	0.001093	639.66	640.21	1.8606	0.001177	906.42	908.77	2.4473
0.01	0.000999	0.01	0.51	0.0000	0.000999	0.03	2.03	0.0001
20	0.001002	83.91	84.41	0.2965	0.001001	83.82	85.82	.2962
40	0.001008	167.47	167.98	0.5722	0.001007	167.29	169.30	.5716
60	0.001017	251.00	251.51	0.8308	0.001016	250.73	252.77	.8300
80	0.001029	334.73	335.24	1.0749	0.001028	334.38	336.44	1.0739
100	0.001043	418.80	419.32	1.3065	0.001043	418.36	420.45	1.3053
120	0.001060	503.37	503.90	1.5273	0.001059	502.84	504.96	1.5259
140	0.001080	588.66	589.20	1.7389	0.001079	588.02	590.18	1.7373
160	—	—	—	—	0.001101	674.14	676.34	1.9410
180	—	—	—	—	0.001127	761.46	763.71	2.1382
200	—	—	—	—	0.001156	850.30	852.61	2.3301
5000 kPa (263.99°C)								
Sat	0.001286	1147.78	1154.21	2.9201	0.001452	1393.00	1407.53	3.3595
0	0.000998	0.03	5.02	0.0001	0.000995	0.10	10.05	0.0003
20	0.001000	83.64	88.64	0.2955	0.000997	83.35	93.32	0.2945
40	0.001006	166.93	171.95	0.5705	0.001003	166.33	176.36	0.5685
60	0.001015	250.21	255.28	0.8284	0.001013	249.34	259.47	0.8258
80	0.001027	333.69	338.83	1.0719	0.001025	332.56	342.81	1.0687
100	0.001041	417.50	422.71	1.3030	0.001039	416.09	426.48	1.2992
120	0.001058	501.79	507.07	1.5232	0.001055	500.07	510.61	1.5188
140	0.001077	586.74	592.13	1.7342	0.001074	584.67	595.40	1.7291
160	0.001099	672.61	678.10	1.9374	0.001195	670.11	681.07	1.9316
180	0.001124	759.62	765.24	2.1341	0.001120	756.63	767.83	2.1274
200	0.001153	848.08	853.85	2.3254	0.001148	844.49	855.97	2.3178
220	0.001187	938.43	944.36	2.5128	0.001181	934.07	945.88	2.5038
240	0.001226	1031.34	1037.47	2.6978	0.001219	1025.94	1038.13	2.6872
260	0.001275	1127.92	1134.30	2.8829	0.001265	1121.03	1133.68	2.8698
280					0.001322	1220.90	1234.11	3.0547
300					0.001397	1328.34	1342.31	3.2468
10000 kPa (311.06°C)								

Compressed Liquid Water

Temp. (°C)	v (m ³ /kg)	u (kJ/kg)	h (kJ/kg)	s (kJ/kg-K)	v (m ³ /kg)	u (kJ/kg)	h (kJ/kg)	s (kJ/kg-K)
15000 kPa (342.24°C)					20000 kPa (365.81°C)			
Sat.	0.001658	1585.58	1610.45	3.6847	0.002035	1785.47	1826.18	4.0137
0	0.000993	0.15	15.04	0.0004	0.000990	0.20	20.00	0.0004
20	0.000995	83.05	97.97	0.2934	0.000993	82.75	102.61	0.2922
40	0.001001	165.73	180.75	0.5665	0.000999	165.15	185.14	0.5646
60	0.001011	248.49	263.65	0.8231	0.001008	247.66	267.82	0.8205
80	0.001022	331.46	346.79	1.0655	0.001020	330.38	350.78	1.0623
100	0.001036	414.72	430.26	1.2954	0.001034	413.37	434.04	1.2917
120	0.001052	498.39	514.17	1.5144	0.001050	496.75	517.74	1.5101
140	0.001071	582.64	598.70	1.7241	0.001068	580.67	602.03	1.7192
160	0.001092	667.69	684.07	1.9259	0.001089	665.34	687.11	1.9203
180	0.001116	753.74	770.48	2.1209	0.001112	750.94	773.18	2.1146
200	0.001143	841.04	858.18	2.3103	0.001139	837.70	860.47	2.3031
220	0.001175	929.89	947.52	2.4952	0.001169	925.89	949.27	2.4869
240	0.001211	1020.82	1038.99	2.6770	0.001205	1015.94	1040.04	2.6673
260	0.001255	1114.59	1133.41	2.8575	0.001246	1108.53	1133.45	2.8459
280	0.001308	1212.47	1232.09	3.0392	0.001297	1204.69	1230.62	3.0248
300	0.001377	1316.58	1337.23	3.2259	0.001360	1306.10	1333.29	3.2071
320	0.001472	1431.05	1453.13	3.4246	0.001444	1415.66	1444.53	3.3978
340	0.001631	1567.42	1591.88	3.6545	0.001568	1539.64	1571.01	3.6074
360					0.001823	1702.78	1739.23	3.8770
30000 kPa					50000 kPa			
0	0.000986	0.25	29.82	0.0001	0.000977	0.20	49.03	-0.0014
20	0.000989	82.16	111.82	0.2898	0.000980	80.98	130.00	0.2847
40	0.000995	164.01	193.87	0.5606	0.000987	161.84	211.20	0.5526
60	0.001004	246.03	276.16	0.8153	0.000996	242.96	292.77	0.8051
80	0.001016	328.28	358.75	1.0561	0.001007	324.32	374.68	1.0439
100	0.001029	410.76	441.63	1.2844	0.001020	405.86	456.87	1.2703
120	0.001044	493.58	524.91	1.5017	0.001035	487.63	539.37	1.4857
140	0.001062	576.86	608.73	1.7097	0.001052	569.76	622.33	1.6915
160	0.001082	660.81	693.27	1.9095	0.001070	652.39	705.91	1.8890
180	0.001105	745.57	778.71	2.1024	0.001091	735.68	790.24	2.0793
200	0.001130	831.34	865.24	2.2892	0.001115	819.73	875.46	2.2634
220	0.001159	918.32	953.09	2.4710	0.001141	904.67	961.71	2.4419
240	0.001192	1006.84	1042.60	2.6489	0.001170	990.69	1049.20	2.6158
260	0.001230	1097.38	1134.29	2.8242	0.001203	1078.06	1138.23	2.7860
280	0.001275	1190.69	1228.96	2.9985	0.001242	1167.19	1229.26	2.9536
300	0.001330	1287.89	1327.80	3.1740	0.001286	1258.66	1322.95	3.1200
320	0.001400	1390.64	1432.63	3.3538	0.001339	1353.23	1420.17	3.2867
340	0.001492	1501.71	1546.47	3.5425	0.001403	1451.91	1522.07	3.4556
360	0.001627	1626.57	1675.36	3.7492	0.001484	1555.97	1630.16	3.6290
380	0.001869	1781.35	1837.43	4.0010	0.001588	1667.13	1746.54	3.8100

Appendix C: Simple derivations

5.2 Water jet

Derivation of travel distance:

At $t = 0$ we get that $x = 0$, which eliminate constant from the integration (Eq. 5.23)

$$x = u \cdot t \cdot \cos \alpha$$

Motion in the vertical direction is defined as:

$$\frac{d^2z}{dt^2} = -g$$

By integration:

$$\frac{dz}{dt} = -gt + c$$

Where c is a constant from the integration. At $t = 0$, $c = u \cdot \sin \alpha$ which leads to:

$$\frac{dz}{dt} = u \cdot \sin \alpha - g \cdot t$$

When $t = 0$, $z = 0$ we get:

$$z = u \cdot t \cdot \sin \alpha - \frac{1}{2} \cdot g \cdot t^2$$

When the jet reaches ground floor $t = t$, $z = 0$:


$$t = 2 \frac{u \cdot \sin \alpha}{g}$$


The horizontal distance travelled is therefor

$$x = \frac{u^2 \cdot \sin^2 \alpha}{g}$$

Appendix D: Hydrostatic test

Test procedure

INTERNAL TEST FORM			 TDW Offshore Services		
<h2>Test procedure</h2> <h3>Hydrostatic Projectile Test</h3>					
Printed by: ABN			Date: 25.05.2016		
Performed by: _____ <small>(Date and sign.)</small>			Approved by: _____ <small>(Date and sign.) (Must be qualified acc. Qual. Matrix)</small>		
Document no. 195243					
Item description: 194778 HYDROSTATIC PROJECTILE TEST ASSEMBLY					
Test info: Test pressure: 30-220 Bar Risk Level: Extra High Force on End Plate: 25 tons					
2	Released	19.05.2016	ABN	EIS	THB
1	Issued for review	19.05.2016	ABN	EIS	THB
Revision	Description	Date	By	Checked	Approved

 TDW Offshore Services	Test procedure Hydrostatic Projectile Test	Page	Revision
		2 of 4	2
		Prepared by	Date
		ABN	25.05.2016

1. PURPOSE OF THE TEST

The purpose of this test is to determine the amount of potential energy stored in a pressurized vessel and transferred into kinetic energy, if a test rig failure occurs. The test is part of a Master thesis written for TDW Offshore Services. The conclusions from the test will be used as basis for determining the specification of safety barriers for upcoming pressure tests at TDW's workshop facility in Stavanger.

2. TEST REQUIREMENTS

Pressure inside vessel should be gradually increased until ejection of the projectile.

At no stage shall the vessel be approached for close examination while it is under pressure.

Drawing 195222 PROJECTILE TEST BRYNE defines the danger area all personnel shall avoid when the test rig is being pressurized.


If desired pressure is not reached, the vessel shall be depressurized before any leak check can start.

Ensure that the projectile have a free path and that any objects that can be hit is removed.

Ricochet effects shall be evaluated.

Chinese fingers to be used to secure hose to fixed point.

Un-expected results from the first two tests shall be taken into consideration before the test sequences can proceed.

 TDW Offshore Services	Test procedure Hydrostatic Projectile Test	Page 3 of 4	Revision 2
		Prepared by ABN	Date 25.05.2016

3. TEST PROCEDURE

1. Verify that the responsible person assembling the test equipment is approved according to the Qualification Matrix. Minimum level 2.

Sign: *[Signature]*



2. Safe job analyses done.



3. Test drawings:



Drawing number: 194778
Revision number: 2

Drawing number: 195222
Revision number: 1

4. Test equipment:



Transmitter: Serial or certificate no.: K216-00029

Manometer: Pressure range (bar): 0-250 BAR

Datalogger: SN 8820

5. Ensure that the test rig and all test equipment is installed according to 195222 PROJECTILE TEST BRYNE



6. Fill the test rig with water through the Projectile opening and make sure there is no air trapped inside.



7. Assemble the projectile and test rig according to 194778 HYDROSTATIC PROJECTILE TEST ASSEMBLY. (Start with one brass pin in the 3mm hole to fasten the Projectile)




8. Lift the 194778 Hydrostatic Test Rig into the test rig 124096 and make sure the 194778 Hydrostatic Test Rig is supported and stabilized and leveled with 1/2in NPT nozzle on top.



9. Mechanically secure the 194778 Hydrostatic Test Rig due to low mass of Hydrostatic Test Rig vs. Projectile



 TDW Offshore Services	Test procedure Hydrostatic Projectile Test	Page	Revision
		4 of 4	2
		Prepared by	Date
		ABN	25.05.2016

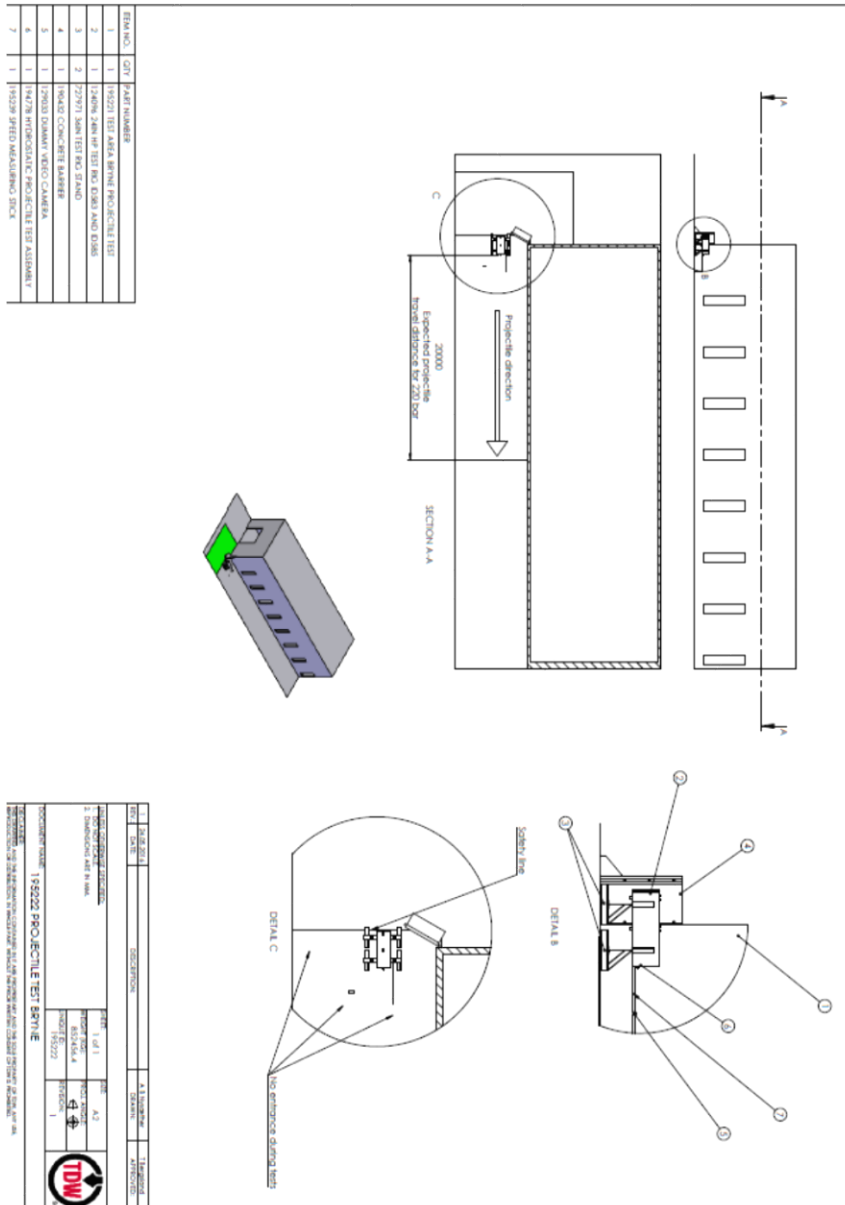
10. Ensure that the projectile will have a free path when it is released.
11. Start the camera.
12. Ensure that all personnel is behind the safety caution line.
13. Regardless of test numbers in Table 1, do not pressurize the test rig more then 220 Bar.
14. Start pressurizing the test rig according to table 1. For each new test points 6-11 shall be repeated.

Test no.	Start@bar	Time	Stop@bar	Comments
1	~30-40	-	Apply pressure until burst, or max 220 bar	1 brass bolt
2	~60-80	-	Apply pressure until burst, or max 220 bar	2 brass bolts
3	~90-120	-	Apply pressure until burst, or max 220 bar	3 brass bolts
4	~120-160	-	Apply pressure until burst, or max 220 bar	4 brass bolts
5	~150-200	-	Apply pressure until burst, or max 220 bar	5 brass bolts
6	~180-220	-	Apply pressure until burst, or max 220 bar	6 brass bolts
7	~200-220	-	Apply pressure until burst, or max 220 bar	7 brass bolts
8	~220-220	-	Apply pressure until burst, or max 220 bar	8 brass bolts

Table 1

REMARKS

Outlay of the testing area for projectile discharge



ITEM NO.	QTY	PART NUMBER
1	1	195221 TEST AREA BURNING PROJECTILE TEST
2	1	124096 24IN HP TEST PIG (300) AND O/S&S
3	2	122971 30IN TEST PIG STAND
4	1	129633 CONCRETE BARREL
5	1	129633 DAMMAY VIDEO CAMERA
6	1	194278 HYDROSTATIC PROJECTILE TEST ASSEMBLY
7	1	195229 SPEED MEASURING DEVICE

REV	DATE	DESCRIPTION	BY	CHKD
1	06/11	195222 PROJECTILE TEST BURNING		

PROJECT NUMBER	195222 PROJECTILE TEST BURNING
PROJECT TITLE	PROJECTILE TEST BURNING
PROJECT NO.	195222
PROJECT CODE	1

DATE	06/11
BY	AK
CHKD	AK
PROJECT NO.	195222
PROJECT CODE	1

Properties brass

Free-Cutting Brass, UNS C36000

COMPONENT	WT. %
C	60 - 63
Fe	Max 0.35
Other	Max 0.5
Pb	2.5 - 3.7
Zn	35.5

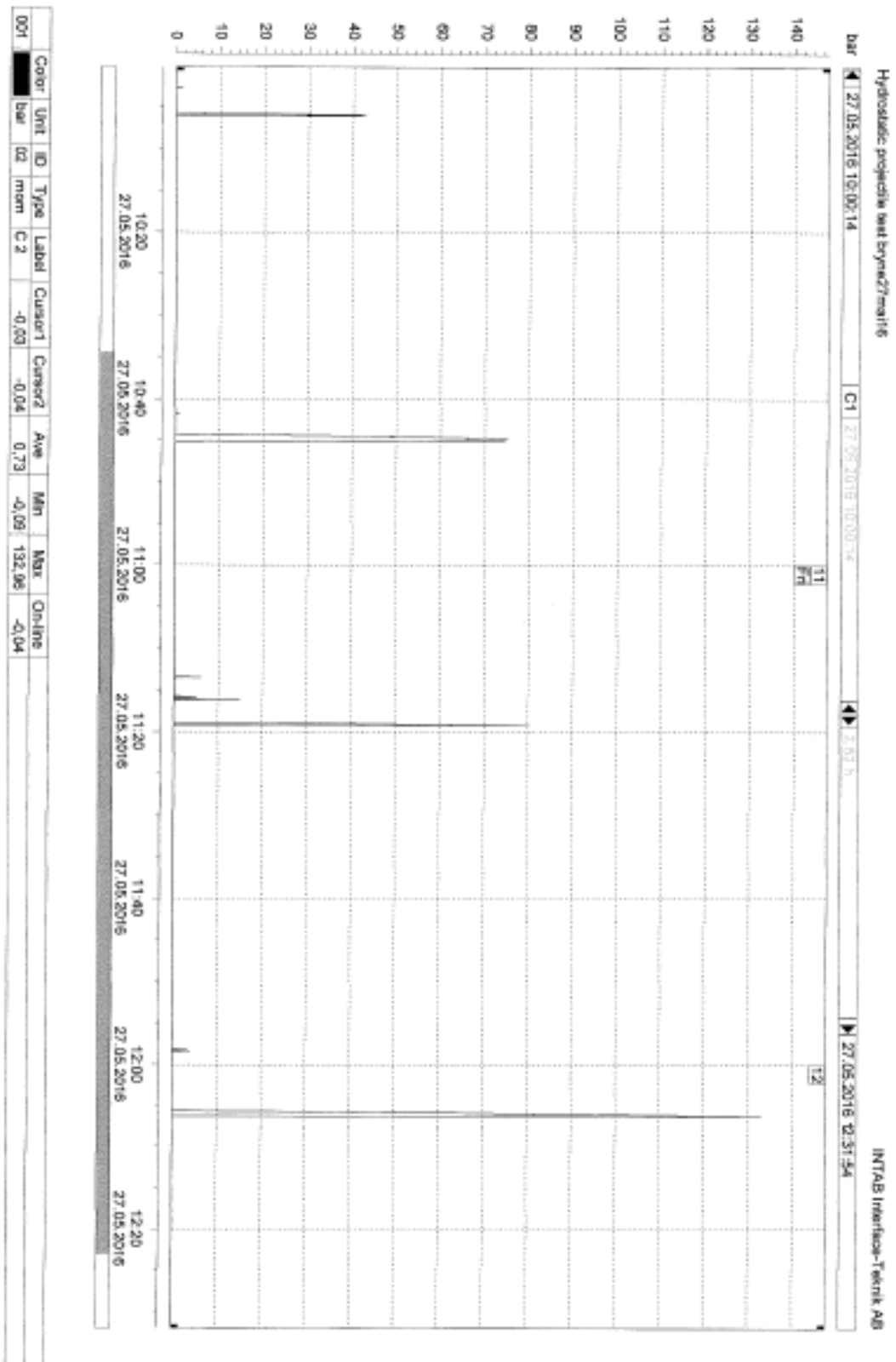
PHYSICAL PROPERTIES	METRIC	ENGLISH	COMMENTS
Density	8.49 g/cc	0.307 lb/in ³	at 20°C (68°F)

MECHANICAL PROPERTIES	METRIC	ENGLISH	COMMENTS
Tensile Strength, Ultimate	338 - 469 MPa	49000 - 68000 psi	
Tensile Strength, Yield	124 - 310 MPa	18000 - 45000 psi	Depending on temper
Elongation at Break	53%	53%	in 457.2 mm
Modulus of Elasticity	97 GPa	14100 ksi	
Bulk Modulus	140 GPa	20300 ksi	Typical for Steel
Poisson's Ratio	0.31	0.31	Calculated
Machinability	100%	100%	UNS C36000 (free-cutting brass) = 100%
Shear Modulus	37 GPa	5370 ksi	

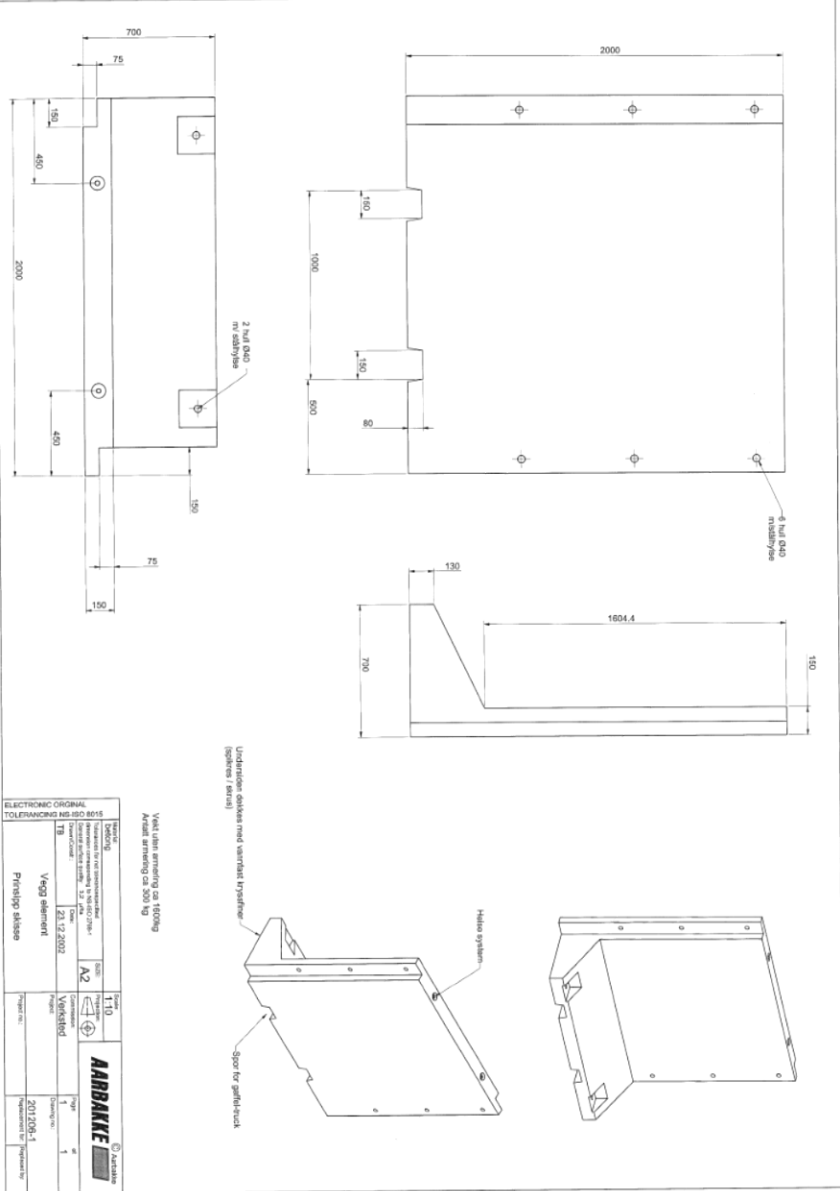
THERMAL PROPERTIES	METRIC	ENGLISH	COMMENTS
CTE, linear 250°C	20.5 µm/m-°C	11.4 µin/in-°F	from 20-300°C (68-570°F)
Thermal Conductivity	115 W/m-K	798 BTU-in /hr-ft ² -°F	at 20°C (68°F)
Melting Point	885 - 900 °C	1630 - 1650 °F	
Solidus	885 °C	1630 °F	
Liquidus	900 °C	1650 °F	



Datalog from test



Appendix E: Existing safety walls

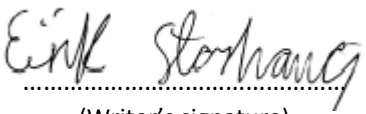


Appendix F: Pre-study report



Faculty of Science and Technology

PRE-STUDY REPORT FOR MASTER THESIS

Study program/Specialization: Construction and Materials Offshoreconstructions	Vårsemesteret, 2016 <u>Open</u> / Restricted access
Writer: Eirik Storhaug	 (Writer's signature)
Faculty supervisor: Hirpa G. Lemu External supervisor(s): Arne B. Nysæther	
Thesis title: Optimal design for projectile and blast protection during pressure testing	
Credits (ECTS): 30 poeng	
Key words:	Pages: 7 Stavanger, 09.02/2016

1 Preface

This pre-study report starts with an introduction of the background behind the project. The introduction will also cover the aim of the project, scope of work and limitations. The project starts at 01. February 2016 and the submission date is 15. June 2016.

The thesis will be written at UiS and the research is conducted in collaboration with TDW Offshore Services who defined the research problem.

The rest of the report will cover the different stages during the project life cycle. This is illustrated with a Work breakdown structure (WBS) and a Gantt-chart will present the time schedule.

2 Contents

<u>1</u>	<u>Introduction</u>	1
1.1	<u>Background</u>	1
1.2	<u>The aim of the Master thesis</u>	1
1.3	<u>Scope of work</u>	1
1.4	<u>Limitations</u>	1
1.5	<u>Report structure</u>	1
<u>2</u>	<u>Short description of the sections</u>	2
2.1	<u>Work breakdown structure (WBS) and Gantt chart</u>	2
2.2	<u>Planning</u>	2
2.3	<u>Pre-study report</u>	2
2.4	<u>Literature study</u>	2
2.5	<u>Calculation</u>	2
2.6	<u>Analyzing different barrier concepts</u>	2
2.7	<u>Develop optimal concept</u>	2
2.8	<u>Publishing</u>	2
<u>3</u>	<u>Work breakdown structure (WBS)</u>	3
<u>4</u>	<u>Time overview</u>	4
4.1	<u>Time schedule</u>	4
4.2	<u>Gantt chart</u>	4
<u>5</u>	<u>Literature list</u>	Feil! Bokmerke er ikke definert.

3 Introduction

3.1 Background

During pressure testing using pressurized vessels on a workshop floor, the surrounding areas need protection, due to the possibility of test failure. A result of failure could be high-pressure water jet or discharge of a projectile. A permanent shield may provide the protection or barrier as part of the test bay design, but since the installation and removal of test vessels is done by crane or forklift. Therefore part of the shield should for practical reasons be made portable. The safety walls should be made of reinforced concrete blocks or section of walls. The walls and blocks have limitations to width, height and weight, and made portable by crane or forklift.

3.2 The aim of the Master thesis

Since there is not any calculations done regarding the safety installments already in place, the thesis will analyze the forces and risks involved in case of failure. Further, the thesis should decide if barriers are sufficient as protection. Based on these results, the thesis will develop an optimal design of barriers necessary for protection during pressure testing. The wall is required to provide a suitable and acceptable protection against potential incidents. The thesis will also investigate if the walls are destroyed or reusable in case of failure.

3.3 Scope of work

- Study codes, regulations and legislation regarding pressure testing. Mainly documents regarding hydro testing of pipelines.
- Calculation of energy during pressure testing and effects of failure.
- Calculations of barriers sufficient as protection.
- Develop concept designs of barriers.
- Producing guidelines for using the barriers.

3.4 Limitations

- Weight and size limitation (thickness, width, height), as the walls should be portable.
- Cost

3.5 Report structure

The report will consist of a title page, which is standard from the University of Stavanger. Then an abstract will follow. The preface should give information about the aim of the thesis, the background for the thesis, the main content of the thesis and acknowledgements to associates. After the preface, there will be contents. Following, there is a summary of the thesis. The summary contains the thesis aim more precisely, the scope of the thesis and which methods utilized during the thesis. The summary also include the most important results, which conclusions made and plans for further work. After the summary, there is an introduction. This tells the approach used in the thesis, its limitations and a disposition of the report. The next section of the thesis is the main part. This starts with theory and regulations, followed by calculations and force analysis. Based on the results there is a conclusion. Here the results are collected and given comments. The conclusion explains what the thesis have accomplished, what deductions made during the report and suggestions for further work. The last part of the thesis is references and attachments.

4 Short description of the sections

4.1 Work breakdown structure (WBS) and Gantt chart

A Work breakdown structure provides the project scope of work, while a Gantt chart shows the project schedule. These are presented later in the report. This chapter will present short the main parts of the content of the thesis.

4.2 Planning

The planning of the master thesis began in November 2015. First, there was an informative meeting with the introduction of subjects for the master thesis and of different supervisors. In December 2015, there was a meeting with TDW Offshore Services about their prospects and goals for the thesis. This meeting was to clarify the ramifications as well as sorting out the logistics in the execution phase of the thesis.

4.3 Pre-study report

The pre-study report introduces the thesis by presenting the aims of the thesis, the scope of work and its limitations. The pre-study report also gives a prospect of the project content and schedule by use of WBS and Gantt chart.

4.4 Literature study

Find relevant literature and regulations regarding pressure testing. Do research on different concepts within pressure testing, as well as other fields of pressure protection e.g. tanks and bomb shelters. Contact companies that conduct pressure testing and compare the safety for the pressure testing areas.

4.5 Calculation

Calculate the forces that are present during a pressure test, and identify dangers during failure. Analyze the dangers and calculate the impact forces for the different failure scenarios. Calculate and simulate with the current safety installment.

4.6 Analyzing different barrier concepts

Introduce different barrier concepts and simulate with the forces calculated in the previous chapter. Define the different advantages and disadvantages of each concept. This chapter will include calculation of strength, pressure containment and cost for the concepts presented. To compare with the calculations, there will also be a practical drop test of a projectile on test material if this is possible. Other factors to consider are mobility of the walls and if they are able to withstand more than one failure.

4.7 Develop optimal concept

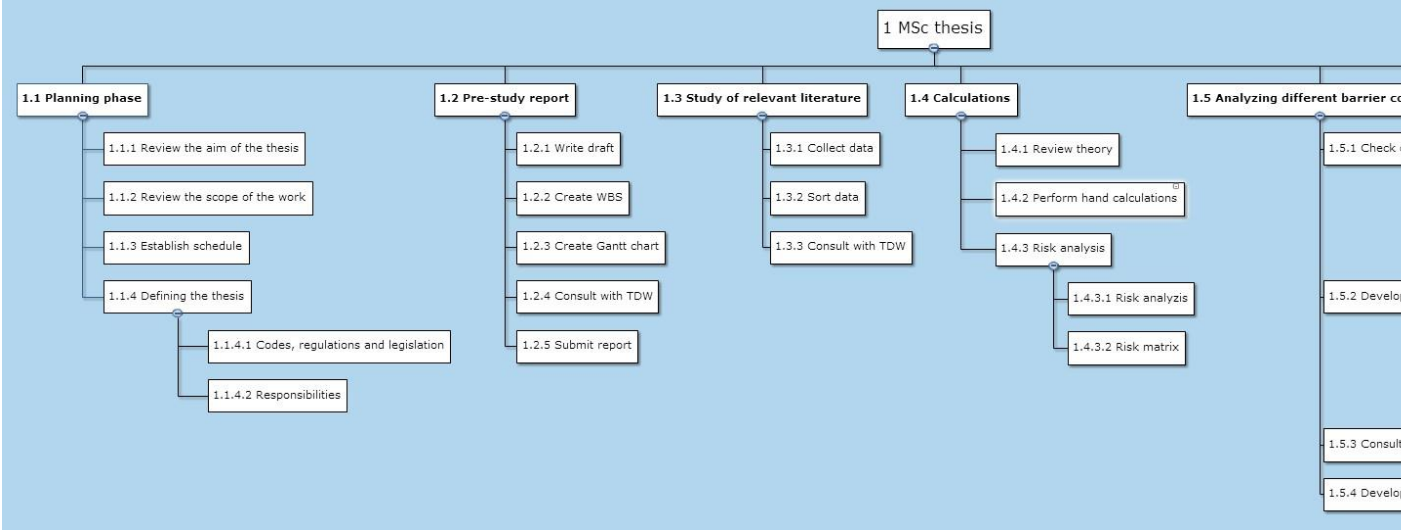
Based on the previous chapter, this chapter presents the chosen concept. It will explain the reason for the choice and give guidelines on how to use the barriers correctly.

4.8 Publishing

This section is for final editing of the thesis, before submission and publishing of the report.

During every phase above, there will be a draft. This will be put together in the last section for final editing. There might be changes in the setup of the thesis.

5 Work breakdown structure (WBS)



6 Time overview

6.1 Time schedule

Order	Activity	Start date	Duration	End date
1	Planning meeting	8. des.	1	9. des.
2	Pre-study report	1. feb.	14	15. feb.
3	Study of relevant literature	10. feb.	29	10. mar.
4	Calculations	1. mar.	40	10. apr.
5	Analyzing different barrier concepts	1. apr.	44	15. mai.
6	Writing the thesis	10. feb.	100	20. mai.
7	Publishing	20. mai.	26	15. jun.

6.2 Gantt chart

